Chapter 26

Gravitational Waves and Experimental Tests of General Relativity

Version 0426.1.pdf, 18 May 2005.
Please send comments, suggestions, and errata via email to kip@tapir.caltech.edu or on paper to Kip Thorne, 130-33 Caltech, Pasadena CA 91125

26.1 Introduction

In 1915, when Einstein formulated general relativity, human technology was incapable of providing definitive experimental tests of his theory. Only a half century later did technology begin to catch up. In the remaining 35 years of the century, experiments improved from accuracies of a few tens of per cent to a part in 1000 or even 10,000; and general relativity passed the tests with flying colors. In Sec. 26.2 we shall describe some of these tests, derive general relativity's predictions for them, and discuss the experimental results.

In the early twenty-first century, observations of gravitational waves will radically change the character of research on general relativity. They will produce, for the first time, tests of general relativity in strong-gravity situations. They will permit us to study relativistic effects in neutron-star and black-hole binaries with exquisite accuracies. They will enable us to map the spacetime geometries of black holes with high precision, and study observationally the large-amplitude, highly nonlinear vibrations of curved spacetime that occur when two black holes collide and merge. And (as we shall see in Chap. 27), they may enable us to probe the singularity in which the universe was born and the universe's evolution in its first tiny fraction of a second.

In this chapter we shall develop the theory of gravitational waves in much detail and shall describe the efforts to detect the waves and the sources that may be seen. More specifically, in Sec. 26.3 we shall develop the mathematical description of gravitational waves, both classically and quantum mechanically (in the language of gravitons), and shall study their propagation through flat spacetime and also, via the tools of geometric optics, through curved spacetime. Then in Sec. 26.4 we shall develop the simplest approximate method for

computing the generation of gravitational waves, the "quadrupole-moment formalism"; and we shall describe and present a few details of other, more sophisticated and accurate methods based on multipolar expansions, post-Newtonian techniques, and numerical simulations on supercomputers ("numerical relativity"). In Sec. 26.5, we shall turn to gravitational-wave detection, focusing especially on detectors such as LIGO and LISA that rely on laser interferometry.

26.2 Experimental Tests of General Relativity

In this section we shall describe briefly some of the most important experimental tests of general relativity. For greater detail, see Will (1993, 2001, 2005)

26.2.1 Equivalence Principle, Gravitational redshift, and Global Positioning System

A key aspect of the equivalence principle is the prediction that all objects, whose size is extremely small compared to the radius of curvature of spacetime and on which no non-gravitational forces act, should move on geodesics. This means, in particular, that their trajectories through spacetime should be independent of their chemical composition. This is called the *weak equivalence principle* or the *universality of free fall*. Efforts to test the universality of free fall date back to Galileo's (perhaps apocryphal) experiment of dropping objects from the leaning tower of Pisa. In the twentieth century a sequence of ever-improving experiments led by Roland von Eötvös (1920), Robert Dicke (1964), Vladimir Braginsky (1972), and Eric Adelberger (1994) have led to an accuracy $\Delta a/a < 5 \times 10^{-13}$ for the difference of gravitational acceleration toward the Sun for earth-bound bodies with very different chemical composition. A proposed space experiment called *STEP* has the prospect to increase this accuracy to the phenomenal level of $\Delta a/a \lesssim 1 \times 10^{-18}$.

General relativity predicts that bodies with significant self gravity (even black holes) should also fall, in a nearly homogeneous external gravitational field, with the same acceleration as a body with negligible self gravity. This prediction has been tested by comparing the gravitational accelerations of the Earth and Moon toward the Sun. Their fractional difference of acceleration [as determined by tracking the relative motions of the Moon and Earth using laser beams fired from Earth, reflected off mirrors that astronauts and cosmonauts have placed on the moon, and received back at earth] has been measured by the *LURE* Project to be $\Delta a/a \lesssim 3 \times 10^{-13}$. Since the Earth and Moon have (gravitational potential energy)/(rest-mass energy) $\simeq -5 \times 10^{-10}$ and $\simeq -2 \times 10^{-10}$ respectively, this verifies that gravitational energy falls with the same acceleration as other forms of energy to within about a part in 1000. For references and for discussions of a variety of other tests of the Equivalence Principle, see Will (1993, 2001, 2005).

From the equivalence principle, one can deduce that, for an emitter and absorber at rest in a Newtonian gravitational field Φ, light (or other electromagnetic waves) must be gravitationally redshifted by an amount $\Delta\lambda/\lambda = \Delta\Phi$, where $\Delta\Phi$ is the difference in Newtonian potential between the locations of the emitter and receiver. (See Ex. 25.5 for a general

relativistic derivation when the field is that of a nonspinning, spherical central body with the emitter on the body's surface and the receiver far from the body.) Relativistic effects will produce a correction to this shift with magnitude $\sim (\Delta\Phi)^2$ [cf. Eq. (25.54)], but for experiments performed in the solar system, the currently available precision is too poor to see this correction; so such experiments test the equivalence principle and not the details of general relativity.

The highest precision test of this gravitational redshift thus far was NASA's 1976 Gravity-Probe-B Project (led by Robert Vessot), in which several atomic clocks were flown to a height of about 10,000 km above the earth, and were compared with atomic clocks on the earth via radio signals transmitted downward. After correcting for special relativistic effects due to the relative motions of the rocket's clocks and the earth clocks, the measured gravitational redshift agreed with the prediction to within the experimental accuracy of about 2 parts in 10,000.

The Global Positioning System (GPS), by which one can determine one's location on Earth to within an accuracy of about 10 meters, is based on signals transmitted from a set of earth-orbiting satellites. Each satellite's position is encoded on its transmitted signals, together with the time of transmission as measured by atomic clocks onboard the satellite. A person's GPS receiver contains a high-accuracy clock and a computer. It measures the signal arrival time and compares with the encoded transmission time to determine the distance from satellite to receiver; and it uses that distance, for several satellites, together with the encoded satellite positions, to determine (by triangulation) the receiver's location on earth.

The transmission times encoded on the signals are corrected for the gravitational redshift before transmission. Without this redshift correction, the satellite clocks would quickly get out of synchronization with all the clocks on the ground, thereby eroding the GPS accuracy; see Ex. 26.1. Thus, a good understanding of general relativity was crucial to the design of the GPS![1]

26.2.2 Perihelion advance of Mercury

It was known at the end of the 19'th century that the point in Mercury's orbit closest to the Sun, known as its perihelion, advances at a rate of about $575''$ per century with respect to the fixed stars, of which about $532''$ can be accounted for by Newtonian perturbations of the other planets. The remaining $\sim 43''$ per century was a mystery until Einstein showed that it can be accounted for quantitatively by the general theory of relativity.

More specifically (as is demonstrated in Ex. 26.2), if we idealize the Sun as nonrotating and spherical so its external gravitational field is Schwarzschild, and we ignore the presence of the other planets, and we note that the radius of Mercury's orbit is very large compared to the Sun's mass (in geometrized units), then Mercury's orbit will be very nearly an ellipse; and the ellipse's perihelion will advance, from one orbit to the next, by an angle

$$\Delta\phi = 6\pi M/p + \mathcal{O}(M^2/p^2) \quad \text{radians}. \tag{26.1}$$

Here M is the Sun's mass and p is the ellipse's *semi latus rectum*, which is related to its semimajor axis a (half its major diameter) and its eccentricity e by $p = a(1 - e^2)$. For the

[1]For further details of the GPS see http://www.BeyondDiscovery.org

parameters of Mercury's orbit ($M = M_\odot \simeq 1.4766$ km, $a = 5.79089 \times 10^7$ km, $e = 0.205628$), this advance is $0.10352''$ per orbit. Since the orbital period is 0.24085 Earth years, this shift corresponds to 42.98 arc seconds per century.

Although the Sun is not precisely spherical, its tiny gravitational oblateness (as inferred from measurements of its spectrum of pulsations; Fig. 15.2) has been shown to contribute negligibly to this perihelion shift; and the frame dragging due to the Sun's rotational angular momentum is also (sadly!) negligible compared to the experimental accuracy; so $42.98''$ per century would be the shift if the Sun and Mercury were the only objects in the solar system. The gravitational fields of the other planets, however, tug on Mercury's orbit, producing—according to Newtonian theory—the large additional shift of about $532''$ per century. The weakness of gravity in the solar system guarantees that relativistic corrections to this additional shift are negligible, and that this shift can be added linearly to the Schwarzschild prediction of $42.98''$, to within the accuracy of the measurements. When this is done and comparison is made with experiment, the $42.98''$ prediction agrees with the observations to within the data's accuracy of about 1 part in 1000.

26.2.3 Gravitational deflection of light, Fermat's Principle and Gravitational Lenses

Einstein not only explained the anomalous perihelion shift of Mercury. He also predicted [Ex. 26.3] that the null rays along which starlight propagates will be deflected, when passing through the curved spacetime near the Sun, by an angle

$$\Delta\phi = 4M/b + \mathcal{O}(M^2/b^2) \,, \tag{26.2}$$

relative to their trajectories if spacetime were flat. Here M is the Sun's mass and b is the ray's impact parameter (distance of closest approach to the Sun's center). For comparison, theories that incorporated a Newtonian-like gravitational field into special relativity (Sec. 24.1) predicted half this deflection. The deflection was measured to an accuracy ~ 20 per cent cent during the 1919 solar eclipse and agreed with general relativity rather than the competing theories—a triumph that helped make Einstein world famous. Modern experiments, based on the deflection of radio waves from distant quasars, as measured using Very Long Baseline Interferometry (interfering the waves arriving at radio telescopes with transcontinental or transworld separations; Sec. 8.3), have achieved accuracies of about 1 part in 10,000, and they agree completely with general relativity. Similar accuracies are now achievable using optical interferometers in space, and may soon be achievable via optical interferometry on the ground.

These accuracies are so great that, when astronomers make maps of the sky using either radio interferometers or optical interferometers, they must now correct for gravitational deflection of the rays *not only when the rays pass near the sun, but for rays coming in from nearly all directions*. This correction is not quite as easy as Eq. (26.2) suggests, since that equation if valid only when the telescope is much farther from the Sun than the impact parameter. In the more general case, the correction is more complicated, and must include aberration due to the telescope motion as well as the effects of spacetime curvature.

As we discussed in Sec. 6.6, the gravitational deflection of light rays (or radio rays) passing through or near a cluster of galaxies can produce a spectacular array of distorted images of the light source. In Chap. 6 we deduced the details of this *gravitational lens effect* using a model in which we treated spacetime as flat, but endowed with a refractive index $n(\mathbf{x}) = 1-2\Phi(\mathbf{x})$, where $\Phi(\mathbf{x})$ is the Newtonian gravitational potential of the lensing system. This model can also be used to compute light deflection in the solar system. We shall now derive this model from general relativity:

The foundation for this model is the following general relativistic version of *Fermat's Principle* [see Eq. (6.42) for the Newtonian version]: Consider any static spacetime geometry, i.e. one for which one can introduce a coordinate system in which $\partial g_{\alpha\beta}/\partial t = 0$ and $g_{jt} = 0$; so the only nonzero metric coefficients are $g_{00}(x^j)$ and $g_{0i}(x^j)$. In such a spacetime the time coordinate t is very special, since it is tied to the spacetime's temporal symmetry. An example is Schwarzschild spacetime and the Schwarzschild time coordinate t. Now, consider a light ray emitted from a spatial point $x^j = a^j$ in the static spacetime and received at a spatial point $x^j = b^j$. Assuming the spatial path along which the ray travels is $x^j(\eta)$ where η is any parameter with $x^j(0) = a^j$, $x^j(1) = b^j$, then the total coordinate time Δt required for the light's trip from a^j to b^j (as computed from the fact that the ray must be null so $ds^2 = g_{00}dt^2 + g_{ij}dx^i dx^j = 0$) is

$$\Delta t = \int_0^1 \sqrt{\gamma_{jk}\frac{dx^j}{d\eta}\frac{dx^k}{d\eta}}d\eta \ , \quad \text{where} \quad \gamma_{jk} \equiv \frac{g_{jk}}{-g_{00}} \ . \tag{26.3}$$

Fermat's principle says that *the actual spatial trajectory of the light path is the one that extremizes this coordinate time lapse.*

To prove this version of Fermat's principle, notice that the action (26.3) is the same as that [Eq. (24.30)] for a geodesic in a 3-dimensional space with metric γ_{jk} and with t playing the role of proper distance traveled. Therefore, the Euler-Lagrange equation for Fermat's action principle $\delta\Delta t = 0$ is the geodesic equation in that space [Eq. (24.26)] with t the affine parameter, which [using Eq. (23.37) for the connection coefficients] can be written in the form

$$\gamma_{jk}\frac{d^2x^k}{dt^2} + \frac{1}{2}(\gamma_{jk,l} + \gamma_{jl,k} - \gamma_{kl,j})\frac{dx^k}{dt}\frac{dx^j}{dt} = 0 \ . \tag{26.4}$$

Next, take the geodesic equation (24.26) for the light ray in the real spacetime, with spacetime affine parameter ζ, and change parameters to t, thereby obtaining

$$\begin{aligned} &g_{jk}\frac{d^2x^k}{dt^2} + \Gamma_{jkl}\frac{dx^k}{dt}\frac{dx^l}{dt} - \Gamma_{j00}\frac{g_{kl}}{g_{00}}\frac{dx^k}{dt}\frac{dx^l}{dt} + \frac{d^2t d\zeta^2}{(dt/d\zeta)^2}g_{jk}\frac{dx^k}{dt} = 0 \ , \\ &\frac{d^2t/d\zeta^2}{(dt/d\zeta)^2} + 2\Gamma_{0k0}\frac{dx^k/dt}{g_{00}} = 0 \ . \end{aligned} \tag{26.5}$$

Insert the second of these equations into the first and write the connection coefficients in terms of derivatives of the spacetime metric. Then with a little algebra you can bring the result into the form (26.4) of the Fermat-principle Euler equation. *Therefore, the null geodesics of spacetime, when viewed as trajectories through the 3-space of constant t, are*

precisely the Fermat-principle paths, i.e. geodesics in a 3-space with metric γ_{jk} and proper-distance affine parameter t. QED

The index-of-refraction formalism used to study gravitational lenses in Chap. 6 is easily deduced as a special case of this Fermat Principle: In a nearly Newtonian situation, the linearized-theory, Lorentz-gauge, trace-reversed metric perturbation has the form (24.107) with only the time-time component being significantly large: $\bar{h}_{00} = -4\Phi$, $\bar{h}_{0j} \simeq 0$, $\bar{h}_{jk} \simeq 0$. Correspondingly, the metric perturbation [obtained by inverting Eq. (24.101)] is $h_{00} = -2\Phi$, $h_{jk} = -\delta_{jk}\Phi$, and the full spacetime metric $g_{\mu\nu} = \eta_{\mu\nu} + h_{\mu\nu}$ is

$$ds^2 = -(1 + 2\Phi)dt^2 + (1 - 2\Phi)\delta_{jk}dx^j dx^k \ . \tag{26.6}$$

This is the standard spacetime metric (24.95) in the Newtonian limit, with a special choice of spatial coordinates, those of linearized-theory Lorentz gauge. The Newtonian limit includes the slow-motion constraint that time derivatives of the metric are small compared to spatial derivatives [Eq. (24.88)], so on the timescale for light to travel through a lensing system, the Newtonian potential can be regarded as static, $\Phi = \Phi(x^j)$. Therefore the Newtonian-limit metric (26.6) is static, and the coordinate time lapse along a trajectory between two spatial points, Eq. (26.3), reduces to

$$\Delta t = \int_0^1 (1 - 2\Phi)d\ell \ , \tag{26.7}$$

where $d\ell = \sqrt{\delta_{jk}dx^j dx^k}$ is distance traveled treating the coordinates as though they were Cartesian, in flat space. This is precisely the action for the Newtonian version of Fermat's Principle, Eq. (6.42), with index of refraction

$$n(x^j) = 1 - 2\Phi(x^j) \ . \tag{26.8}$$

Therefore, the spatial trajectories of the light rays can be computed via the Newtonian Fermat Principle, with the index of refraction (26.8). *QED*

Although this index-of-refraction model involves treating a special (Lorentz-gauge) coordinate system as though the spatial coordinates were Cartesian and space were flat (so $d\ell^2 = \delta_{jk}dx^j dx^k$)— which does not correspond to reality—, nevertheless, this model predicts the correct gravitational lens images. The reason is that it predicts the correct rays through the Lorentz-gauge coordinates, and when the light reaches Earth, the cumulative lensing has become so great that the fact that the coordinates here are slightly different from truly Cartesian has negligible influence on the images one sees.

26.2.4 Shapiro time delay

In 1964 Irwin Shapiro proposed a new experiment to test general relativity: Monitor the round-trip travel time for radio waves transmitted from earth and bounced off Venus or some other planet, or transponded by a spacecraft. As the line-of-sight between the Earth and the planet or spacecraft gradually moves nearer then farther from the Sun, the waves' rays will pass through regions of greater or smaller spacetime curvature, and this will influence the round-trip travel time by greater or smaller amounts. From the time evolution of the round-trip time, one can deduce the changing influence of the Sun's spacetime curvature.

One can compute the round-trip travel time with the aid of Fermat's Principle. The round-trip proper time, as measured on Earth (neglecting, for simplicity, the Earth's orbital motion; i.e., pretending the Earth is at rest relative to the Sun while the light goes out and back) is $\Delta\tau_\oplus = \sqrt{1-2M/r_\oplus}\,\Delta t \simeq (1-M/r_\oplus)\Delta t$, where M is the Sun's mass, $r_\oplus$ is the Earth's distance from the Sun's center, Δt is the round-trip coordinate time in the static solar-system coordinates, and we have used $g_{00} = 1-2M/r_\oplus$. Because Δt obeys Fermat's Principle, it is stationary under small perturbations of the the light's spatial trajectory. This allows us to compute it using a straight-line trajectory through the spatial coordinate system. Letting b be the impact parameter (the ray's closest coordinate distance to the Sun) and x be coordinate distance along the straight-line trajectory and neglecting the gravitational fields of the planets, we have $\Phi = -M/\sqrt{x^2+b^2}$, so the coordinate time lapse out and back is

$$\Delta t = 2\int_{-\sqrt{r_\oplus^2-b^2}}^{\sqrt{r_{\rm refl}^2-b^2}} \left(1+\frac{2M}{\sqrt{x^2+b^2}}\right) dx\ . \tag{26.9}$$

Here $r_{\rm refl}$ is the radius of the location at which the light gets reflected (or transponded) back to Earth. Performing the integral and multiplying by $\sqrt{g_{00}} \simeq 1-M/r_\oplus$, we obtain for the round-trip travel time measured on Earth

$$\Delta\tau_\oplus = 2\,(a_\oplus + a_{\rm refl})\left(1-\frac{M}{r_\oplus}\right) + 4M\ln\left[\frac{(a_\oplus+r_\oplus)(a_{\rm refl}+r_{\rm refl})}{b^2}\right]\ , \tag{26.10}$$

where $a_\oplus = \sqrt{r_\oplus^2-b^2}$ and $a_{\rm refl} = \sqrt{r_\oplus^2-b^2}$.

As the Earth and the reflecting planet or transponding spacecraft move along their orbits, only one term in this round-trip time varies sharply: the term

$$4M\ln(1/b^2) = 8M\ln b \simeq 40\mu{\rm s}(b/R_\odot)\ . \tag{26.11}$$

When the planet or spacecraft passes nearly behind the Sun, as seen from Earth, b plunges to a minimum (on a timescale of hours or days) then rises back up, and correspondingly the time delay shows a sharp blip. By comparing the observed blip with the theory in a measurement with the Cassini spacecraft, this Shapiro time delay has been verified to the remarkable precision of about 1 part in 100,000 (Bertotti, Iess and Tortora 2003).

26.2.5 Frame dragging and Gravity Probe B

As we have discussed in Secs. 24.9.3 and 25.5, the rotational angular momentum $\mathbf{J}$ of a gravitating body places its imprint on the body's asymptotic spacetime metric:

$$ds^2 = -\left(1-\frac{2M}{r}\right)dt^2 - \frac{4\epsilon_{jkm}J^k x^m}{r^3}dtdx^j + \left(1+\frac{2M}{r}\right)\delta_{jk}dx^j dx^k\ . \tag{26.12}$$

Here, for definiteness, we are using Lorentz gauge, and M is the body's mass; cf. Eq. (24.112). The angular-momentum term drags inertial frames into rotation about the body (Sec. 25.2). One manifestation of this frame dragging is a precession of inertial-guidance gyroscopes near the body. Far from the body, a gyroscope's spin axis will remain fixed relative to distant galaxies and quasars, but near the body it will precess.

It is easy to deduce the precession in the simple case of a gyroscope whose center of mass is at rest in the coordinate system of Eq. (26.12), i.e. at rest relative to the body. The transport law for the gyroscope's spin is $\nabla_{\vec{u}}\vec{S} = \vec{u}(\vec{a}\cdot\vec{S})$ [Eq. (23.90) boosted from special relativity to general relativity via the equivalence principle]. Here $\vec{u}$ is the gyroscope's 4-velocity (so $u^j = 0$, $u^0 = 1/\sqrt{1-2M/r} \simeq 1 + M/r \simeq 1$) and $\vec{a}$ its 4-acceleration. The spatial components of this transport law are

$$S^j{}_{,t}u^0 \simeq S^j{}_{,t} = -\Gamma^j{}_{k0}S^k u^0 \simeq -\Gamma^j{}_{k0}S^k \simeq -\Gamma_{jk0}S^k \simeq \frac{1}{2}(g_{0k,j} - g_{0j,k})S^k \ . \tag{26.13}$$

Here each $\simeq$ means "is equal, up to fractional corrections of order M/r". By inserting g_{j0} from the line element (26.12) and performing some manipulations with Levi-Civita tensors, we can bring Eq. (26.13) into the form

$$\frac{\partial \mathbf{S}}{\partial t} = \mathbf{\Omega}_{\rm prec} \times \mathbf{S} \ , \quad \text{where} \quad \mathbf{\Omega}_{\rm prec} = \frac{1}{r^3}[-\mathbf{J} + 3(\mathbf{J}\cdot\mathbf{n})\mathbf{n}] \ . \tag{26.14}$$

Here $\mathbf{n} = \mathbf{e}_{hatr}$ is the unit radial vector pointing away from the gravitating body. Equation (26.14) says that the gyroscope's spin angular momentum rotates (precesses) with angular velocity $\mathbf{\Omega}_{\rm prec}$ in the coordinate system (which is attached to distant inertial frames, i.e. to the distant galaxies and quasars). This is sometimes called a "gravitomagnetic precession" because the off-diagonal term g_{j0} in the metric, when thought of as a 3-vector, is $-4\mathbf{J}\times\mathbf{n}/r^2$, which has the same form as the vector potential of a magnetic dipole; and the gyroscopic precession is similar to that of a magnetized spinning body interacting with that magnetic dipole.

In magnitude, the precessional angular velocity (26.14) in the vicinity of the Earth is roughly one arcsec per century, so measuring it is a tough experimental challenge. A team led by Francis Everitt has designed and constructed a set of superconducting gyroscopes that are currently (2005) flying in an Earth-orbiting satellite called Gravity Probe B, with the goal of measuring this precession to a precision of about 1 part in 100 (see http://einstein.stanford.edu/).

26.2.6 Binary Pulsar

Gravity in the solar system is very weak. Even at Mercury's orbit, the gravitational potential of the Sun is only $|\Phi| \sim 3\times10^{-8}$. Therefore, when one expands the spacetime metric in powers of Φ, current experiments with their fractional accuracies $\sim 10^{-4}$ or worse are able to see only the first-order terms beyond Newtonian theory; i.e. terms of *first post-Newtonian order*. To move on to second post-Newtonian order, $\mathcal{O}(\Phi^2)$ beyond Newton, will require major advances in technology, or observations of astronomical systems in which Φ is far larger than 3×10^{-8}.

Radio observations of binary pulsars (this subsection) provide one opportunity for such observations; gravitational-wave observations of neutron-star and black-hole binaries (Sec. 26.5) provide another.

The best binary pulsar for tests of general relativity is PSR1913+16, discovered by Russell Hulse and Joseph Taylor in 1974. This system consists of two neutron stars in a mutual

elliptical orbit with period $P \sim 8$ hr and eccentricity $e \sim 0.6$. One of the stars emits pulses at a regular rate. These are received at earth with time delays due to crossing the binary orbit and other relativistic effects. We do not know *a priori* the orbital inclination or the neutron-star masses. However, we obtain one relation between these three quantities by analyzing the Newtonian orbit. A second relation comes from measuring the consequences of the combined second order Doppler shift and gravitational redshift as the pulsar moves in and out of its companion's gravitational field. A third relation comes from measuring the relativistic precession of the orbit's periastron (analog of the perihelion shift of Mercury). (The precession rate is far larger than for Mercury: about 4° per year!) From these three relations one can solve for the stars' masses and the orbital inclination, and as a check can verify that the Shapiro time delay comes out correctly. One can then use the system's parameters to predict the rate of orbital inspiral due to gravitational-radiation reaction—a phenomenon with magnitude $\sim |\Phi|^{2.5}$ beyond Newton, i.e. 2.5 post-Newtonian order (Sec. 26.4.2 below). The prediction agrees with the measurements to accuracy ~ 0.1 per cent (Weissberg and Taylor 2004) —a major triumph for general relativity!

****

EXERCISES

Exercise 26.1 *Practice: Gravitational Redshift for Global Positioning System*
The GPS satellites are in circular orbits at a height of 18,000 km above the Earth's surface. If the ticking rates of the clocks on the satellites were not corrected for the gravitational redshift, roughly how long would it take them to accumulate a time shift, relative to clocks on the earth, large enough to degrade the GPS position accuracy by 10 meters? by 1 kilometer?

Exercise 26.2 *Example: Perihelion Shift*
Consider a small satellite in non-circular orbit about a spherical body with much larger mass M, for which the external gravitational field is Schwarzschild. The satellite will follow a timelike geodesic. Orient the Schwarzschild coordinates so the satellite's orbit is in the equatorial plane, $\theta = \pi/2$.

(a) Because the metric coefficients are independent of t and ϕ, the quantities $\tilde{E} = -p_t$ and $\tilde{L} = p_\phi$ must be constants of the satellite's motion [cf. Ex. 24.4]. Show that

$$\tilde{E} = \left(1 - \frac{2M}{r}\right)\frac{dt}{d\tau} ,$$
$$\tilde{L} = r^2 \frac{d\phi}{d\tau} . \tag{26.15}$$

Explain why $\tilde{E}$ has the physical interpretation of the satellite's orbital energy per unit mass (including rest-mass energy) and why $\tilde{L}$ is its angular momentum per unit mass.

(b) Introduce the coordinate $u = r^{-1}$ and use the normalization of the 4-velocity to derive the following differential equation for the orbit:

$$\left(\frac{du}{d\phi}\right)^2 = \frac{\tilde{E}^2}{\tilde{L}^2} - \left(u^2 + \frac{1}{\tilde{L}^2}\right)(1 - 2Mu) \ . \tag{26.16}$$

(c) Differentiate this equation with respect to ϕ to obtain a second order differential equation

$$\frac{d^2u}{d\phi^2} + u - \frac{M}{\tilde{L}^2} = 3Mu^2. \tag{26.17}$$

By reinstating the constants G, c, and comparing with the Newtonian orbital equation, argue that the right-hand side represents a relativistic perturbation to the Newtonian equation of motion.

(e) Assume, henceforth in this exercise, that $r \gg M$ (i.e. $u \ll 1/M$), and solve the orbital equation (26.17) by perturbation theory. More specifically: At zero order (i.e., setting the right side to zero), show that the Kepler ellipse

$$u_K = \left(\frac{M}{\tilde{L}^2}\right)(1 + e\cos\phi), \tag{26.18}$$

is a solution. Here e (a constant of integration) is the ellipse's eccentricity and $\tilde{L}^2/M$ is the ellipse's *semi latus rectum*. The orbit has its minimum radius at $\phi = 0$.

(f) By substituting u_K into the right hand side of the relativistic equation of motion (26.17), show (at first-order in the relativistic perturbation) that in one orbit the angle ϕ at which the satellite is closest to the mass advances by $\Delta\phi \simeq 6\pi M^2/\tilde{L}^2$. (Hint: Try to write the differential equation in the form $d^2u/d\phi^2 + (1+\epsilon)^2 u \simeq \ldots$, where $\epsilon \ll 1$.)

(g) For the planet Mercury, the orbital period is $P = 0.241$ yr and the eccentricity is $e = 0.206$. Deduce that the relativistic contribution to the rate of advance of the *perihelion* (point of closest approach to the Sun) is $43''$ per century.

Exercise 26.3 *Example: Gravitational Deflection of Light.*
Repeat the previous exercise for a photon following a null geodesic.

(a) Show that the trajectory obeys the differential equation

$$\frac{d^2u}{d\phi^2} + u = 3Mu^2 \ . \tag{26.19}$$

(b) Obtain the zero'th order solution by ignoring the right hand side,

$$u = \frac{\sin\phi}{b} \ . \tag{26.20}$$

where b is an integration constant. Show that, in the asymptotically flat region far from the body, this is just a straight line and b is the impact parameter (distance of closest approach to the body).

(c) Substitute this solution into the right hand side and show that the perturbed trajectory satisfies

$$u = \frac{\sin\phi}{b} + \frac{M}{b^2}(1-\cos\phi)^2 \ . \tag{26.21}$$

(d) Hence show that a ray with impact parameter $b \gg M$ will be deflected through an angle

$$\alpha = \frac{4M}{b} \ ; \tag{26.22}$$

cf. Eq. (6.77) and associated discussion.

****

26.3 Gravitational Waves and their Propagation[2]

26.3.1 The gravitational wave equation

Gravitational waves are *ripples in the curvature of spacetime* that are emitted by violent astrophysical events, and that propagate out from their sources with the speed of light. It was clear to Einstein and others, even before general relativity was fully formulated, that his theory would have to predict gravitational waves; and within months after completing the theory, Einstein (1916, 1918) worked out the basic properties of those waves.

It turns out that, after they have been emitted, gravitational waves propagate through matter with near impunity, i.e., they propagate as though in vacuum, even when other matter and fields are present. (For a proof and discussion see, e.g., Sec. 2.4.3 of Thorne, 1983). This justifies simplifying our analysis to vacuum propagation. By contrast with most texts on gravitational waves, we shall *not* further simplify to propagation through a spacetime that is flat, aside from the waves, because it is almost as easy to analyze propagation through a curved background spacetime as a flat one.

The key to the analysis is the same two-lengthscale expansion as underlies geometric optics for any kind of wave propagating through any kind of medium (Sec. 6.3): We presume that the waves' reduced wavelength $\lambda\!\!\!^{-}$ (wavelength/2π) as measured in some relevant local Lorentz frame is very short compared to the radius of curvature of spacetime $\mathcal{R} \sim 1/\sqrt{R_{\hat\alpha\hat\beta\hat\gamma\hat\delta}}$ and the lengthscale $\mathcal{L}$ on which the background curvature changes (e.g., the radius of the Earth when the waves are near Earth):

$$\lambda\!\!\!^{-} \ll \{\mathcal{R}, \mathcal{L}\} \tag{26.23}$$

cf. Eq. (6.16). Then the Riemann curvature tensor can be split into two pieces: The background curvature $R^{\rm B}_{\alpha\beta\gamma\delta}$, which is the average of Riemann over a few wavelengths, plus the waves' curvature $R^{\rm GW}_{\alpha\beta\gamma\delta}$, which is the remaining, oscillatory piece:

$$R_{\alpha\beta\gamma\delta} = R^{\rm B}_{\alpha\beta\gamma\delta} + R^{\rm GW}_{\alpha\beta\gamma\delta} \ , \quad R^{\rm B}_{\alpha\beta\gamma\delta} \equiv \langle R_{\alpha\beta\gamma\delta}\rangle \ . \tag{26.24}$$

[2]MTW, Sec. 18.2 and Chap. 35, 36, 37; Thorne (1983, 1987).

This is the same kind of split as we used in developing the quasilinear theory of plasma waves (Sec. 22.2.1). Similarly, we can split the spacetime metric into a sum of a smooth background part plus a gravitational-wave perturbation, denoted $h_{\alpha\beta}$

$$g_{\alpha\beta} = g^{\rm B}_{\alpha\beta} + h_{\alpha\beta}\ ; \quad \text{where} \quad g^{\rm B}_{\alpha\beta} = \langle g_{\alpha\beta}\rangle\ . \tag{26.25}$$

Obviously, the smooth background Riemann tensor $R^{\rm B}_{\alpha\beta\gamma\delta}$ can be computed in the usual manner from the smooth background metric $g^{\rm B}_{\alpha\beta}$.

Because the waves are generally very weak, we can regard their metric perturbation $h_{\alpha\beta}$ and Riemann tensor $R^{\rm GW}_{\alpha\beta\gamma\delta}$ as linearized fields that live in the smooth, curved background spacetime. When we do so, we can replace gradients (subscript ";") based on the full physical metric $g_{\alpha\beta}$ by gradients (subscript "|") based on the background metric so, e.g., $R^{\rm GW}_{\alpha\beta\gamma\delta;\mu} = R^{\rm GW}_{\alpha\beta\gamma\delta|\mu}$. This linearization implies that the waves' Riemann tensor can be computed from their metric perturbation via

$$R^{\rm GW}_{\alpha\beta\gamma\delta} = \frac{1}{2}(h_{\alpha\delta|\beta\gamma} + h_{\beta\gamma|\alpha\delta} - h_{\alpha\gamma|\beta\delta} - h_{\beta\delta|\alpha\gamma})\ , \tag{26.26}$$

as one can see from the fact that this formula reduces to the right result, Eq. (24.96), in a local Lorentz frame of the background metric. We shall use the waves' Riemann tensor $R^{GW}_{\alpha\beta\gamma\delta}$ as our primary entity for describing the waves, and shall use the metric perturbation only as a computational tool—mostly when analyzing wave generation.

Notice that the combination of indices that appears on the right side of Eq. (26.26) is carefully designed to produce an entity with the symmetries of Riemann

$$R_{\alpha\beta\gamma\delta} = -R_{\beta\alpha\gamma\delta}\ , \quad R_{\alpha\beta\gamma\delta} = -R_{\alpha\beta\delta\gamma}\ , \quad R_{\alpha\beta\gamma\delta} = R_{\gamma\delta\alpha\beta}\ . \tag{26.27}$$

[Eq. (24.52)]. This combination of indices is encountered frequently in gravitational-wave theory, so it is useful to introduce the following short-hand notation for it:

$$S_{\{\alpha\beta\gamma\delta\}} \equiv S_{\alpha\delta\beta\gamma} + S_{\beta\gamma\alpha\delta} - S_{\alpha\gamma\beta\delta} - S_{\beta\delta\alpha\gamma}\ . \tag{26.28}$$

In terms of this notation, expression (26.26) reads

$$R^{\rm GW}_{\alpha\beta\gamma\delta} = \frac{1}{2}h_{\{\alpha\beta|\gamma\delta\}}\ . \tag{26.29}$$

One benefit of the two-lengthscale condition $\lambda\!\!\!^{-} \ll \mathcal{R}$ is the fact that the double gradient of the gravitational waves' Riemann tensor is far larger than the product of the waves' Riemann with the background Riemann

$$R^{\rm GW}_{\alpha\beta\gamma\delta|\mu\nu} \sim \frac{R^{\rm GW}_{\alpha\beta\gamma\delta}}{\lambda\!\!\!^{-2}} \gg \frac{R^{\rm GW}_{\alpha\beta\gamma\delta}}{\mathcal{R}^2} \sim R^{\rm GW}_{\alpha\beta\gamma\delta}R^{\rm B}_{\mu\nu\rho\sigma}\ . \tag{26.30}$$

Since the commutator of the double gradient is a sum of products of the wave Riemann with the background Riemann [generalization of Eq. (24.39) with p^α replaced by $R^{\rm GW}_{\alpha\beta\gamma\delta}$], *gradients of* $R^{\rm GW}_{\alpha\beta\gamma\delta}$ *commute to high accuracy*:

$$R^{\rm GW}_{\alpha\beta\gamma\delta|\mu\nu} = R^{\rm GW}_{\alpha\beta\gamma\delta|\nu\mu}\ . \tag{26.31}$$

We shall use this fact in deriving the wave equation for $R^{\rm GW}_{\alpha\beta\gamma\delta}$.

Our derivation of the wave equation will be based on a combination of the Riemann curvature's Bianchi identity

$$R^{\alpha}{}_{\beta\gamma\delta;\epsilon} + R^{\alpha}{}_{\beta\delta\epsilon;\gamma} + R^{\alpha}{}_{\beta\epsilon\gamma;\delta} = 0 \tag{26.32}$$

[Eq. (26.32)] and the vacuum Einstein field equation $G^{\alpha\beta} \equiv R^{\alpha\beta} - \frac{1}{2}Rg^{\alpha\beta} = 0$. By contracting the vacuum field equation on its two slots, we find that the scalar curvature R vanishes, and by inserting this back into the vacuum field equation we find that the Ricci tensor vanishes:

$$R_{\alpha\beta} \equiv R^{\mu}{}_{\alpha\mu\beta} = 0 \quad \text{in vacuum.} \tag{26.33}$$

By then contracting the Bianchi identity (26.32) on its first and fifth slots and invoking (26.33) we find that the Riemann tensor is divergence-free:

$$R^{\mu}{}_{\beta\gamma\delta;\mu} = 0 \quad \text{in vacuum.} \tag{26.34}$$

The symmetries (26.27) guarantee that *Riemann is divergence-free not only on its first slot, but in fact, on each of its four slots*. By next taking the divergence of the Bianchi identity (26.32) on its last slot, we obtain

$$R_{\alpha\beta\gamma\delta;\mu}{}^{\mu} = -R_{\alpha\beta\delta\mu;\gamma}{}^{\mu} - R_{\alpha\beta\mu\gamma;\delta}{}^{\mu} \ . \tag{26.35}$$

We now split this equation into its rapidly oscillating (wave) piece and its background piece, and for the wave piece we approximate the full-spacetime gradients ";" by background-spacetime gradients "|", we commute the gradient indices on the right-hand side [Eq. (26.31)], and we use the vanishing of the divergence [Eq. (26.34)] to obtain

$$R^{\rm GW}_{\alpha\beta\gamma\delta|\mu}{}^{\mu} = 0 \ . \tag{26.36}$$

This is the wave equation for gravitational waves propagating through the curved, background spacetime. It is a perfect analog of the vacuum wave equation $A_{\alpha;\mu}{}^{\mu} = 0$ [Eq. (24.71)] for electromagnetic waves. Both wave equations dictate that their waves propagate at the speed of light ($c = 1$ in our geometrized units).

To get insight into the waves, we pick a region of spacetime far from the source, where the wavefronts are nearly flat, and in that region we introduce a local Lorentz frame of the background spacetime. This frame must be small compared to the background radius of curvature $\mathcal{R}$; but since $\lambda\!\!\!^{-} \ll \mathcal{R}$, the frame can still be big compared to $\lambda\!\!\!^{-}$. For example, for waves passing near and through Earth, in the frequency band $f \sim 100$ Hz of Earth-based detectors, $\mathcal{R}$ is about 10^9 km and $\lambda\!\!\!^{-}$ is about 500 km, so the local Lorentz frame could be given a size $\sim 10^5$ km (~ 10 times larger than the Earth), which is huge compared to $\lambda\!\!\!^{-}$ but small compared to $\mathcal{R}$.

In this local Lorentz frame, by virtue of Eqs. (24.28) and (26.30), the wave equation (26.36) becomes

$$\left(-\frac{\partial^2}{\partial t^2} + \frac{\partial^2}{\partial x^2} + \frac{\partial^2}{\partial y^2} + \frac{\partial^2}{\partial z^2} \right) R^{\rm GW}_{\alpha\beta\gamma\delta} = 0 \ , \tag{26.37}$$

For simplicity, we orient the spatial axes of the local Lorentz frame so the waves propagate in the z-direction, and we neglect the curvature of the phase fronts (i.e., we treat the waves as planar). Then the solution to (26.37) is an arbitrary function of $t - z$:

$$R^{\rm GW}_{\alpha\beta\gamma\delta} = R^{\rm GW}_{\alpha\beta\gamma\delta}(t - z) \ . \tag{26.38}$$

This shows explicitly that the waves propagate with the speed of light.

26.3.2 The waves' two polarizations: + and ×

In this subsection we shall explore the properties of gravitational waves. Throughout the discussion we shall confine attention to the background's local Lorentz frame, far from the source, in which the waves are nearly planar and have the form (26.38).

Only two of the 20 independent components of $R^{\rm GW}_{\alpha\beta\gamma\delta}$ are independent functions of $t - z$; the other eighteen are determined in terms of those two by the following considerations: (*i*) The Bianchi identity (26.32), when applied to the specific functional form (26.38) and then integrated in time (with the integration constant dropped because we are studying waves that fluctuate in time), implies

$$R^{\rm GW}_{\alpha\beta xy} = 0 \ , \quad R^{\rm GW}_{\alpha\beta xz} = -R^{\rm GW}_{\alpha\beta x0} \ , \quad R^{\rm GW}_{\alpha\beta yz} = -R^{\rm GW}_{\alpha\beta y0} \ . \tag{26.39}$$

(*ii*) This, together with Riemann's symmetries (26.27), implies that all components can be expressed in terms of $R^{\rm GW}_{j0k0}$ (which is general relativity's analog of the Newtonian tidal tensor $\mathcal{E}_{jk}$). (*iii*) The vacuum Einstein equation (26.33) then implies that

$$R^{\rm GW}_{z0z0} = R^{\rm GW}_{z0x0} = R^{\rm GW}_{x0z0} = R^{\rm GW}_{z0y0} = R^{\rm GW}_{y0z0} = 0 \ , \tag{26.40}$$

and

$$R^{\rm GW}_{x0x0} = -R^{\rm GW}_{y0y0} \equiv -\frac{1}{2}\ddot{h}_+(t - z) \ , \quad R^{\rm GW}_{x0y0} = R^{\rm GW}_{y0x0} \equiv -\frac{1}{2}\ddot{h}_\times(t - z) \ . \tag{26.41}$$

Here the two independent components have been expressed in terms of dimensionless functions $h_+(t - z)$ and $h_\times(t - z)$. The double time derivatives, denoted by double dots ($\ddot{h}_+ \equiv \partial^2 h_+/\partial t^2$), are required by dimensionality: Riemann has dimensions of 1/length^2 or equivalently 1/time^2; so if h_+ and $h_\times$ are to be dimensionless, they must be differentiated twice in (26.41). The factors of $\frac{1}{2}$ are relics of the past history of general relativity research.

Equation (26.40) says that for a gravitational wave the space-time-space-time part of Riemann is *transverse*; i.e., it has no spatial components along the propagation direction (z-direction). This is completely analogous to the fact that the electric and magnetic fields of an electromagnetic wave are transverse to the propagation direction. The first of Eqs. (26.41) says that the nonvanishing, transverse-transverse part of Riemann is *traceless*. These two properties are often summarized by saying that gravitational waves are "transverse and traceless," or "TT."

The two independent functions h_+ and $h_\times$ are called the "gravitational-wave fields" for the "+ (plus) polarization state" and for the "× (cross) polarization state."

We can reconstruct all the components of the waves' Riemann tensor from these two gravitational-wave fields as follows: First define the polarization tensors

$$\mathbf{e}^+ \equiv (\vec{e}_x \otimes \vec{e}_x - \vec{e}_y \otimes \vec{e}_y) \ , \quad \mathbf{e}^\times \equiv (\vec{e}_x \otimes \vec{e}_y + \vec{e}_y \otimes \vec{e}_x) \ , \tag{26.42}$$

and a second-rank gravitational-wave field

$$\begin{aligned} &h^{\rm TT}_{\alpha\beta} = h_+ e^+_{\alpha\beta} + h_\times e^\times_{\alpha\beta} \ ; \quad \text{or equivalently} \\ &h^{\rm TT}_{xx} = -h^{\rm TT}_{yy} = h_+ \ , \quad h^{\rm TT}_{xy} = h^{\rm TT}_{yx} = h_+ \ , \quad \text{all other } h^{\rm TT}_{\alpha\beta} \text{ vanish.} \end{aligned} \tag{26.43}$$

[The notation "TT" indicates that this field is transverse to the propagation direction (z-direction) and traceless. The relationship between this $h^{\rm TT}_{\alpha\beta}$ and the metric perturbation $h_{\alpha\beta}$ will be explained in Sec. 26.3.7 below.] Then the waves' Riemann tensor is

$$R^{\rm GW}_{\alpha\beta\gamma\delta} = \frac{1}{2} h^{\rm TT}_{\{\alpha\beta|\gamma\delta\}} \ ; \quad \text{and in particular} \quad R^{\rm GW}_{0j0k} = -\frac{1}{2}\ddot{h}^{\rm TT}_{jk} \ . \tag{26.44}$$

We shall seek physical insight into h_+ and $h_\times$ by studying the following idealized problem: Consider a cloud of test particles that floats freely in space and is static and spherical before the waves pass. We shall study the wave-induced deformations of the cloud as viewed in the nearest thing there is to a rigid, orthonormal coordinate system: the local Lorentz frame (in the physical spacetime) of a "fiducial particle" that sits at the cloud's center. In that frame the displacement vector ξ^j between the fiducial particle and some other particle has components $\xi^j = x^j + \delta x^j$, where x^j is the other particle's spatial coordinate before the waves pass, and δx^j is its coordinate displacement, as produced by the waves. By inserting this into the local-Lorentz-frame variant of the equation of geodesic deviation, Eq. (24.42), and neglecting the tiny δx^k compared to x^k on the right side, we obtain

$$\frac{d^2 \delta x^j}{dt^2} = -R^{\rm GW}_{j0k0} x^k = \frac{1}{2}\ddot{h}^{\rm TT}_{jk} x^k \ , \tag{26.45}$$

which can be integrated twice to give

$$\delta x^j = \frac{1}{2} h^{\rm TT}_{jk} x^k \ . \tag{26.46}$$

The middle expression in Eq. (26.45) is the *gravitational-wave tidal acceleration* that moves the particles back and forth relative to each other. It is completely analogous to the Newtonian tidal acceleration $-R_{j0k0}x^k = -(\partial^2\Phi/\partial x^j \partial x^k)x^k$ by which the moon raises tides on the earth's oceans [Sec. 24.5.1].

Specialize, now, to a wave with + polarization (for which $h_\times = 0$). By inserting expression (26.43) into (26.46), we obtain

$$\delta x = \frac{1}{2} h_+ x \ , \quad \delta y = -\frac{1}{2} h_+ y \ , \quad \delta z = 0 \ . \tag{26.47}$$

This displacement is shown in Fig. 26.1(a,b). Notice that, as the gravitational-wave field h_+ oscillates at the cloud's location, the cloud is left undisturbed in the z-direction (propagation

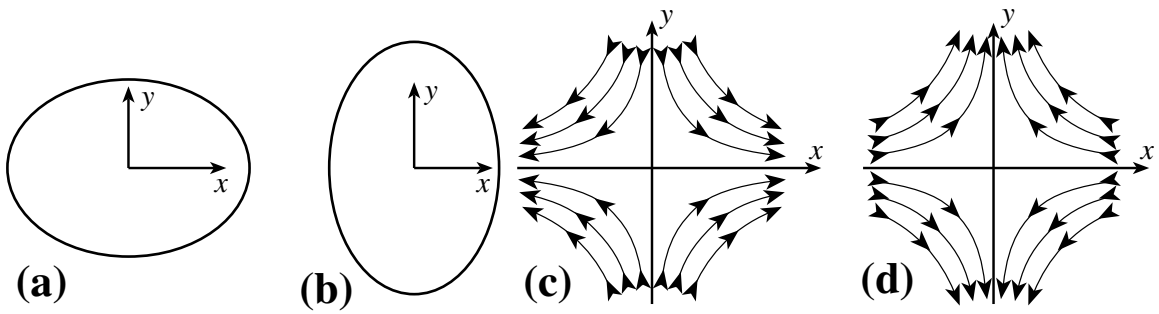

Fig. 26.1: Physical manifestations, in a particle's local Lorentz frame, of h_+ gravitational waves. (a) Transverse deformation of an initially spherical cloud of test particles at a phase of the wave when $h_+ > 0$. (b) Deformation of the cloud when $h_+ < 0$. (c) Field lines representing the acceleration field which produces the cloud's deformation, at a phase when $\ddot{h}_+ > 0$. (d) Acceleration field lines when $\ddot{h}_+ < 0$.

direction), and in transverse planes it gets deformed into an ellipse elongated first along the x-axis (when $h_+ > 0$), then along the y-axis (when $h_+ < 0$). Because $R_{x0x0} = -R_{y0y0}$, i.e., because R_{j0k0} is traceless, the ellipse is squashed along one axis by the same amount as it is stretched along the other, i.e., the area of the ellipse is preserved during the oscillations.

The effects of the h_+ polarization state can also be described in terms of the *tidal acceleration field* that it produces in the central particle's local Lorentz frame:

$$\frac{d^2}{dt^2}\delta\mathbf{x} = \frac{1}{2}\ddot{h}_+(x\mathbf{e}_x - y\mathbf{e}_y) \;, \tag{26.48}$$

where $\ddot{h}_+ \equiv \partial^2 h_+/\partial t^2$. Notice that this acceleration field is divergence free. Because it is divergence-free, it can be represented by lines of force, analogous to electric field lines, which point along the field and have a density of lines proportional to the magnitude of the field; and when this is done, the field lines will never end. Figure 26.1(c,d) shows this acceleration field at the phases of oscillation when $\ddot{h}_+$ is positive and when it is negative. Notice that the field is quadrupolar in shape, with a field strength (density of lines) that increases linearly with distance from the origin of the local Lorentz frame. The elliptical deformations of the sphere of test particles shown in Fig. 26.1(a,b) are the responses of that sphere to this quadrupolar acceleration field. The polarization state which produces these accelerations and deformations is called the + state because of the orientation of the axes of the quadrupolar acceleration field [Fig. 26.1(c,d)].

Turn, next, to the $\times$ polarization state. In this state the deformations of the initially circular ring are described by

$$\delta x = \frac{1}{2}h_\times y \;, \quad \delta y = \frac{1}{2}h_\times x \;, \quad \delta z = 0 \;. \tag{26.49}$$

These deformations, like those for the + state, are purely transverse; they are depicted in Fig. 26.2(a,b). The acceleration field that produces these deformations is

$$\frac{d^2}{dt^2}\delta\mathbf{x} = \frac{1}{2}\ddot{h}_\times(y\mathbf{e}_x + x\mathbf{e}_y) \;. \tag{26.50}$$

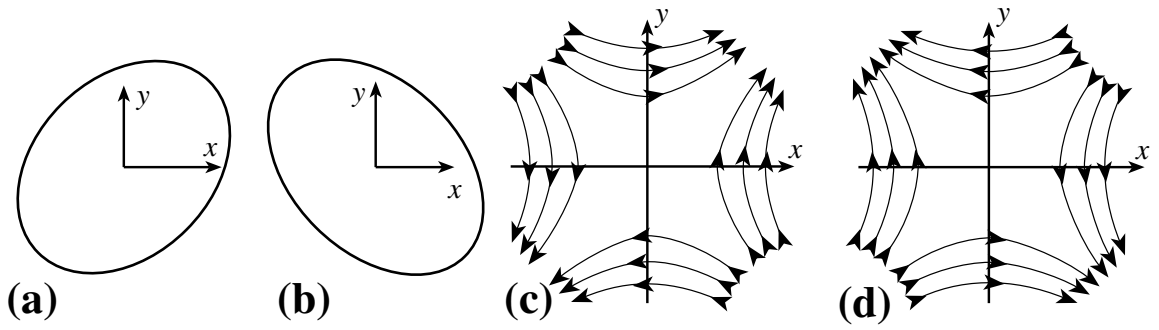

Fig. 26.2: Physical manifestations, in a particle's local Lorentz frame, of $h_\times$ gravitational waves. (a) Deformation of an initially circular sphere of test particles at a phase of the wave when $h_\times > 0$. (b) Deformation of the sphere when $h_\times < 0$. (c) Field lines representing the acceleration field which produces the sphere's deformation, at a phase of the wave when $\ddot{h}_\times > 0$. (d) Acceleration field lines when $\ddot{h}_\times < 0$.

This acceleration field, like the one for the + polarization state, is divergence free and quadrupolar; the field lines describing it are depicted in Fig. 26.2(c,d). The name "× polarization state" comes from the orientation of the axes of this quadrupolar acceleration field.

In defining the gravitational-wave fields h_+ and $h_\times$, we have relied on a choice of (local Lorentz) reference frame, i.e. a choice of local Lorentz basis vectors $\vec{e}_\alpha$. Exercise 26.4 explores how these fields change when the basis is changed. The conclusions are simple: (i) When one rotates the transverse basis vectors $\vec{e}_x$ and $\vec{e}_y$ through an angle ψ, then h_+ and $h_\times$ "rotate" through 2ψ in the sense that:

$$(h_+ + ih_\times)_{\rm new} = (h_+ + ih_\times)_{\rm old} e^{2i\psi} \ , \quad \text{when} \quad (\vec{e}_x + i\vec{e}_y)_{\rm new} = (\vec{e}_x + i\vec{e}_y) e^{i\psi} \ . \tag{26.51}$$

(ii) When one boosts from an old frame to a new one moving at some other speed, but chooses the old and new spatial bases such that (a) the waves propagate in the z direction in both frames and (b) the plane spanned by $\vec{e}_x$ and $\vec{\kappa} \equiv \vec{e}_0 + \vec{e}_z$ =(propagation direction in spacetime) is the same in both frames, then h_+ and $h_\times$ are the same in the two frames—i.e., they are scalars under such a boost!

26.3.3 Gravitons and their spin

Most of the above features of gravitational waves (though not expressed in this language) were clear to Einstein in 1918. Two decades later, as part of the effort to understand quantum fields, M. Fierz and Wolfgang Pauli (1939) at the Eidgenössische Technische Hochschule (ETH) in Zurich, Switzerland formulated a classical theory of linear fields of arbitrary spin so designed that the fields would be quantizable by canonical methods. Remarkably, their canonical theory for a field of spin two is identical to general relativity with nonlinear effects removed, and the plane waves of that spin-two theory are identical to the waves described above. When quantized by canonical techniques, these waves are carried by zero-rest-mass, spin-two gravitons.

One can see by the following simple argument that the gravitons which carry gravitational waves must have spin two: Consider any plane-wave field (neutrino, electromagnetic, gravitational, ...) that propagates at the speed of light in the z-direction of a (local) Lorentz frame. At any moment of time examine any physical manifestation of that field, e.g., the acceleration field it produces on test particles. Rotate that manifestation of the field around the z axis, and ask what is the minimum angle of rotation required to bring the field back to its original configuration. Call that minimum angle, $\theta_{\rm ret}$, the waves' *return angle*. The spin S of the particles that carry the wave will necessarily be related to that return angle by

$$S = \frac{360 \text{ degrees}}{\theta_{\rm ret}} \ . \tag{26.52}$$

This simple formula corresponds to the elegant mathematical statement that "the waves generate an irreducible representation of order $S = 360\,\text{degrees}/\theta_{\rm ret}$ of that subgroup of the Lorentz group which leaves their propagation vector unchanged (the 'Little group' of the rotation vector)." For electromagnetic waves a physical manifestation is the electric field, which is described by a vector lying in the x–y plane; if one rotates that vector about the z-axis (propagation axis), it returns to its original orientation after a return angle $\theta_{\rm ret} = 360$ degrees. Correspondingly, the spin of the particle which carries the electromagnetic wave (the photon) is one. For neutrinos the return angle is $\theta_{\rm ret} = 720$ degrees; and correspondingly the spin of a neutrino is $\frac{1}{2}$. For gravitational waves the physical manifestations include the deformation of a sphere of test particles [Figs. 26.1(a,b) and 26.2(a,b)] and the acceleration fields [Figs. 26.1(c,d) and 26.2(c,d)]. Both the deformed, ellipsoidal spheres and the quadrupolar lines of force return to their original orientations after rotation through $\theta_{\rm ret} = 180$ degrees; and correspondingly, the graviton must have spin two.

Although Fierz and Pauli (1939) showed us how to quantize linearized general relativity, the quantization of full, nonlinear general relativity remains a difficult subject of current research, to which we shall return briefly in the next chapter.

26.3.4 Energy and Momentum in Gravitational Waves

In 1968 Richard Isaacson discovered a beautiful and powerful method to define a stress-energy tensor for a gravitational wave. This method is similar to the one by which we analyzed the back-action of a plasma wave on the plasma's background particle distribution [Eq. (22.4)]. Here, as there, we take our exact dynamical equation (the Einstein field equation here, the Vlasov equation there) and expand it to quadratic order in the wave:

$$G_{\alpha\beta} = G^{\rm B}_{\alpha\beta} + G^{(1)}_{\alpha\beta} + G^{(2)}_{\alpha\beta} = 0 \ . \tag{26.53}$$

In this equation $G_{\alpha\beta}$ is the Einstein tensor for the full spacetime metric $g_{\mu\nu} = g^{\rm B}_{\mu\nu} + h_{\mu\nu}$, $G^{\rm B}_{\alpha\beta}$ is the Einstein tensor for the background metric $g^{\rm B}_{\alpha\beta}$, $G^{(1)}_{\alpha\beta}$ is the part linear in $h_{\mu\nu}$, and $G^{(2)}_{\alpha\beta}$ is the part quadratic in $h_{\mu\nu}$. This is the analog of the quadratically expanded Vlasov equation (22.3). Here, as in the plasma case, we next split our dynamical equation into two parts, its spatial average (which is smooth on the scale $\lambda\!\!\!^{-}$) and its remaining, fluctuating piece. In the plasma case the fluctuating piece is the linear wave equation for the plasma waves; in

the gravitational case it is a variant of the gravitational wave equation $R^{\rm GW}_{\alpha\beta\gamma\delta|\mu}{}^{\mu} = 0$. In the plasma case the averaged piece is Eq. (22.4) by which the waves at quadratic order in their amplitude act back on the unperturbed particle distribution. In the gravitational case, it is the equation

$$G^{\rm B}_{\alpha\beta} = -\langle G^{(2)}_{\alpha\beta}\rangle \ , \tag{26.54}$$

by which the waves at quadratic order produce background spacetime curvature.

Equation (26.54) can be brought into the standard form for Einstein's equation in the background spacetime,

$$G^{\rm B}_{\alpha\beta} = 8\pi T^{\rm GW}_{\alpha\beta} \ , \tag{26.55}$$

by attributing to the waves a stress-energy tensor defined by

$$T^{\rm GW}_{\alpha\beta} = -\frac{1}{8\pi}\langle G^{(2)}_{\alpha\beta}\rangle \ . \tag{26.56}$$

Because this stress-energy tensor involves an average over a few wavelengths, its energy density, momentum density, energy flux, and momentum flux are *not defined* on lengthscales shorter than a wavelength. One cannot say how much energy or momentum resides in the troughs of the waves and how much in the crests. One can only say how much total energy there is in a region containing a few wavelengths. However, once one has reconciled oneself to this amount of nonlocality, one finds that $T^{\rm GW}_{\alpha\beta}$ has all the other properties that one expects of any good stress-energy tensor. Most especially, in the absence of coupling of the waves to matter (the situation we are treating), it obeys the standard conservation law

$$T^{{\rm GW}\,\alpha\beta}{}_{|\beta} = 0 \ . \tag{26.57}$$

This law is a direct consequence of the averaged field equation (26.56) and the contracted Bianchi identity for the background spacetime $G^{{\rm B}\,\alpha\beta}{}_{|\beta} = 0$.

By grinding out the second-order perturbation of the Einstein tensor and inserting it into Eq. (26.56), performing several integrations by parts in the average $\langle \ldots \rangle$, and invoking results to be derived in Sec. 26.3.7, one arrives at the following simple expression for $T^{\rm GW}_{\alpha\beta}$ in terms of the wave fields h_+ and $h_\times$:

$$T^{\rm GW}_{\alpha\beta} = \frac{1}{16\pi}\langle h_{+,\alpha}h_{+,\beta} + h_{\times,\alpha}h_{\times,\beta}\rangle \ . \tag{26.58}$$

[For details of the derivation, see Isaacson (1968) or Secs. 35.13 and 35.15 of MTW.]

Let us examine this stress-energy tensor in the background spacetime's local Lorentz frame, which we used above when exploring the properties of gravitational waves. Because $h_+ = h_+(t-z)$ and $h_\times = h_\times(t-z)$, the only nonzero components of Eq. (26.58) are

$$T^{{\rm GW}\,00} = T^{{\rm GW}\,0z} = T^{{\rm GW}\,z0} = T^{{\rm GW}\,zz} = \frac{1}{16\pi}\langle \dot{h}_+^2 + \dot{h}_\times^2\rangle \kappa_\alpha \kappa_\beta \ . \tag{26.59}$$

This has the same form as the stress-energy tensor for a plane electromagnetic wave propagating in the z direction, and the same form as the stress-energy tensor for any collection of zero-rest-mass particles moving in the z-direction [cf. Eq. (2.46)], as it must since the

gravitational waves are carried by zero-rest-mass gravitons just as electromagnetic waves are carried by zero-rest-mass photons.

Suppose that the waves have frequency $\sim f$ and that the amplitudes of oscillation of h_+ and $h_\times$ are $\sim h_{\rm amp}$ Then by inserting factors of G and c into Eq. (26.59) [i.e., by switching from geometrized units to conventional units] and by setting $\langle(\partial h_+/\partial t)^2\rangle \simeq 1/2(2\pi f h_{\rm amp})^2$ and similarly for $h_\times$, we obtain the following approximate expression for the energy flux in the waves:

$$T^{{\rm GW}\,0z} \simeq \frac{\pi}{4}\frac{c^3}{G^2} f^2 h_{\rm amp}^2 \simeq 300 \frac{\rm ergs}{\rm cm^2\ sec}\left(\frac{f}{1\ {\rm kHz}}\right)^2\left(\frac{h_{\rm amp}}{10^{-21}}\right)^2 . \tag{26.60}$$

The numbers in this equation correspond to a strongly emitting, highly asymmetric supernova in the Virgo cluster of galaxies. Contrast this huge gravity-wave energy flux with the peak electromagnetic flux at the height of the supernova, $\sim 10^{-9}$ erg cm^{-2} sec^{-1}; but note that the gravity waves should last for only a few milliseconds, while the strong electromagnetic output lasts for weeks.

Corresponding to the huge energy flux (26.60) in an astrophysically interesting gravitational wave is a huge *mean occupation number* for the quantum states of the gravitational-wave field, i.e., a huge value for the number of spin-2, zero-rest-mass gravitons in each quantum state. To compute that occupation number, we shall evaluate the volume in phase space occupied by the waves from a supernova and then divide by the volume occupied by each quantum state [cf. Sec. 2.3]. At a time when the waves have reached a distance r from the source, they occupy a spherical shell of area $4\pi r^2$ and thickness of order $10\lambda\!\!\!^{-}$, where $\lambda\!\!\!^{-} = 1/(2\pi f)$ is their reduced wavelength, so their volume in physical space is $\mathcal{V}_x \sim 100 r^2 \lambda\!\!\!^{-}$. As seen by observers whom the waves are passing, they come from a solid angle $\Delta\Omega \sim (2\lambda\!\!\!^{-}/r)^2$ centered on the source, and they have a spread of angular frequencies ranging from $\omega \sim \frac{1}{2}c/\lambda\!\!\!^{-}$ to $\omega \sim 2c/\lambda\!\!\!^{-}$. Since each graviton carries an energy $\hbar\omega = \hbar c/\lambda\!\!\!^{-}$ and a momentum $\hbar\omega/c = \hbar/\lambda\!\!\!^{-}$, the volume that they occupy in momentum space is $\mathcal{V}_p \sim (2\hbar/\lambda\!\!\!^{-})^3\Delta\Omega$, i.e., $\mathcal{V}_p \sim 10\hbar^3/(\lambda r^2)$. The gravitons' volume in phase space, then, is

$$\mathcal{V}_x\mathcal{V}_p \sim 1000\hbar^3 \sim 4(2\pi\hbar)^3 . \tag{26.61}$$

Since each quantum state for a zero rest-mass particle occupies a volume $(2\pi\hbar)^3$ in phase space [Eq. (2.22)], this means that the total number of quantum states occupied by the gravitons is of order unity! Correspondingly, the mean occupation number of each occupied state is of order the total number of gravitons emitted, which (since the total energy radiated in an extremely strong supernova is of order $10^{-2}M_\odot c^2 \sim 10^{52}$ ergs, and each graviton carries an energy $\hbar c/\lambda\!\!\!^{-} \sim 10^{-23}$ erg), is

$$\bar\eta \sim 10^{75} . \tag{26.62}$$

This enormous occupation number means that the waves behave exceedingly classically; quantum-mechanical corrections to the classical theory have fractional magnitude $1/\sqrt{\bar\eta} \sim 10^{-37}$.

26.3.5 Wave propagation in a source's local asymptotic rest frame

Consider a source of gravitational waves somewhere far out in the universe. In the vicinity of the source but some wavelengths away from it (so the waves are well defined), introduce

a local Lorentz reference frame in which the source is at rest: the source's *local asymptotic rest frame*. In that frame construct spherical polar coordinates (t, r, θ, ϕ) centered on the source so the background metric is

$$ds^2 = -dt^2 + dr^2 + r^2(d\theta^2 + \sin^2\theta d\phi^2) \ . \tag{26.63}$$

The wave gravitational wave equation $R_{\alpha\beta\gamma\delta|\mu}{}^{\mu} = 0$ can be solved fairly easily in this coordinate system. The solution has the form that one would expect from experience with scalar waves and electromagnetic waves in spherical coordinates, plus the description of plane gravitational waves in Sec. 26.3.2: The waves propagate radially with the speed of light, so their wave fields h_+ and $h_\times$ are rapidly varying functions of retarded time

$$\tau_r \equiv t - r \ , \tag{26.64}$$

and slowly varying functions of angle (θ, ϕ), and they die out as $1/r$:

$$h_+ = \frac{Q_+(\tau_r; \theta, \phi)}{r} \ , \quad h_\times = \frac{Q_\times(\tau_r; \theta, \phi)}{r} \ . \tag{26.65}$$

These propagation equations can be thought of as saying that Q_+ and $Q_\times$ are constant along radial null rays, i.e. curves of constant $\tau_r = t - r$, θ and ϕ; and h_+ and $h_\times$ are equal to these constantly-propagated Q's, modified by a $1/r$ falloff.

Notice that the null tangent vector to the radial rays is

$$\vec{k} = \vec{e}_t + \vec{e}_r = -\boldsymbol{\nabla}\tau_r \ . \tag{26.66}$$

By a computation in the coordinate basis, one can show that the radius factor r, which appears in the $1/r$ falloff law, evolves along the rays in accord with the equation

$$\nabla_{\vec{k}} r = r_{,\alpha} k^\alpha = \frac{1}{2}(\vec{\nabla} \cdot \vec{k}) r \ , \tag{26.67}$$

This may look like a complicated way to describe r, but its virtue is that, when the waves have left the source's vicinity and are traveling through the real, lumpy universe, the wave fields will continue to have the form (26.65), with r evolving in accord with (26.67)! [Sec. 26.3.6 below].

The wave fields are not fully meaningful until we have specified their associated polarization tensors. Those tensors can be defined along each ray using two transverse, orthonormal polarization vectors, $\vec{a}$ [the analog of $\vec{e}_x$ in Eq. (26.42)] and $\vec{b}$ [the analog of $\vec{e}_y$]:

$$\mathbf{e}^+ = (\vec{a} \otimes \vec{a} - \vec{b} \otimes \vec{b}) \ , \quad \mathbf{e}^\times = (\vec{a} \otimes \vec{b} + \vec{b} \otimes \vec{a}) \ . \tag{26.68}$$

The vectors $\vec{a}$ and $\vec{b}$ must be held constant along each ray, or equivalently must be parallel transported along the rays:

$$\nabla_{\vec{k}} \vec{a} = \nabla_{\vec{k}} \vec{b} = 0 \ . \tag{26.69}$$

It is conventional, in the source's local asymptotic rest frame, to choose

$$\vec{a} = \vec{e}_{\hat{\theta}} \ , \quad \vec{b} = \vec{e}_{\hat{\phi}} \ , \tag{26.70}$$

so the axes for the + polarization are in the θ and ϕ directions, and those for the $\times$ polarization are rotated 45 degrees to $\vec{e}_{\hat{\theta}}$ and $\vec{e}_{\hat{\phi}}$.

Once the polarization tensors have been constructed, and the wave fields (26.65) are known, then the waves' TT gravitational-wave field can be computed from the standard equation

$$h^{\rm TT}_{\alpha\beta} = h_+ e^+_{\alpha\beta} + h_\times e^\times_{\alpha\beta} \tag{26.71}$$

[Eq. (26.43)], and the waves' Riemann tensor can be computed from the obvious generalization of Eq. (26.44):

$$R^{\rm GW}_{\alpha\beta\gamma\delta} \simeq \frac{1}{2} h^{\rm TT}_{\{\alpha\beta|\gamma\delta\}} = \frac{1}{2}\frac{\partial^2 h^{\rm TT}_{\{\alpha\beta}}{\partial\tau_r^2}\frac{\partial\tau_r}{\partial x^\gamma}\frac{\partial\tau_r}{\partial x^{\delta\}}} = \frac{1}{2}\frac{\partial^2 h^{\rm TT}_{\{\alpha\beta}}{\partial\tau_r^2} k_\gamma k_{\delta\}} \ . \tag{26.72}$$

Here the derivative with respect to retarded time τ_r is taken holding (θ, ϕ, r) fixed, and the $\{\ldots\}$ on the indices has the meaning of Eq. (26.28). As an important special case, if the the basis vectors are chosen in the θ and ϕ directions [Eq. (26.70)], then the tide-producing space-time-space-time part of Riemann [Eq. (26.72)] takes form

$$R^{\rm GW}_{\hat{\theta}\hat{0}\hat{\theta}\hat{0}} = -R^{\rm GW}_{\hat{\phi}\hat{0}\hat{\phi}\hat{0}} = \frac{1}{2} h_{+,\tau_r\tau_r} \ , \quad R^{\rm GW}_{\hat{\theta}\hat{0}\hat{\phi}\hat{0}} = R^{\rm GW}_{\hat{\phi}\hat{0}\hat{\theta}\hat{0}} = \frac{1}{2} h_{\times,\tau_r\tau_r} \ , \tag{26.73}$$

which is the obvious generalization of Eq. (26.41) to radially propagating waves.

We shall demonstrate at the end of the next section that the Riemann tensor (26.72) constructed by the above procedure is, indeed, a solution of the gravitational wave equation.

26.3.6 Wave propagation via geometric optics

The two-lengthscale conditions (26.23), which underlie the definition of gravitational waves, permit us to solve the gravitational wave equation $R^{\rm GW}_{\alpha\beta\gamma\delta|\mu}{}^{\mu} = 0$ by means of geometric optics.

We developed the concepts of geometric optics for rather general types of waves in Sec. 6.3. When those techniques are applied to the gravitational wave equation, they reveal that, as the waves travel through our lumpy, bumpy universe, with its stars, galaxies, and black holes, they continue to propagate along null geodesics, just as they did in the local asymptotic rest frame where they originated. Classically the null geodesics are the waves' rays; quantum mechanically they are the world lines of the waves' gravitons. Because electromagnetic waves also propagate along null-geodesic rays (photon world lines), *gravitational waves must exhibit all the same null-ray-induced phenomena as electromagnetic waves: doppler shifts, cosmological redshifts, gravitational redshifts, gravitational deflection of rays, and gravitational lensing.*

Each ray starts out traveling radially through the local asymptotic rest frame, so it can be identified by three parameters: the direction (θ, ϕ) in which it was emitted, and the retarded time τ_r of its emission. The rays carry these three labels out through spacetime with themselves, and in particular they lay down the scalar field $\tau_r(\mathcal{P})$. As in the source's local asymptotic rest frame, so also throughout spacetime, the vector

$$\vec{k} \equiv -\vec{\nabla}\tau_r \tag{26.74}$$

continues to be tangent to the null rays (so $\vec{k}\cdot\vec{k}=0$), and continues to satisfy the null geodesic equation

$$\nabla_{\vec{k}}\vec{k}=0\ , \tag{26.75}$$

as one can see by the following index manipulations:

$$k_{\alpha|\mu}k^\mu=-\tau_{e|\alpha\mu}k^\mu=-\tau_{e|\mu\alpha}k^\mu=k_{\mu|\alpha}k^\mu=\frac{1}{2}(\vec{k}\cdot\vec{k})_{|\alpha}=0\ . \tag{26.76}$$

[Here the second expression follows from the definition (26.74) of $\vec{k}$, the third follows from the fact that double gradients of scalars (by contrast with vectors) commute, the fourth follows from (26.74) again, the fifth from the rule for differentiating products (and the fact that the gradient of the metric vanishes), and the sixth from the fact that $\vec{k}\cdot\vec{k}=0$.] Thus, $\vec{k}\equiv-\vec{\nabla}\tau_r$ continues to be the null-geodesic tangent vector.

As in the source's local asymptotic rest frame, so throughout spacetime: (i) the Q functions Q_+ and $Q_\times$ continue to be constant along each ray, (ii) the radius function r continues to evolve via the propagation law

$$\nabla_{\vec{k}}r=r_{,\alpha}k^\alpha=\frac{1}{2}(\vec{\nabla}\cdot\vec{k})r\ , \tag{26.77}$$

[Eq. (26.67)], (iii) the polarization vectors continue to be parallel transported along the rays

$$\nabla_{\vec{k}}\vec{a}=\nabla_{\vec{k}}\vec{b}=0\ , \tag{26.78}$$

[Eq. (26.69)], and continue to be used to build the polarization tensors via

$$\mathbf{e}^+=(\vec{a}\otimes\vec{a}-\vec{b}\otimes\vec{b})\ ,\quad \mathbf{e}^\times=(\vec{a}\otimes\vec{b}+\vec{b}\otimes\vec{a})\ . \tag{26.79}$$

[Eq. (26.68)], (iv) the gravitational-wave fields continue to be constructed via the equations

$$h_+=\frac{Q_+(\tau_r;\theta,\phi)}{r}\ ,\quad h_\times=\frac{Q_\times(\tau_r;\theta,\phi)}{r}\ , \tag{26.80}$$

$$h^{\rm TT}_{\alpha\beta}=h_+e^+_{\alpha\beta}+h_\times e^\times_{\alpha\beta} \tag{26.81}$$

[Eqs. (26.65) and (26.71)] and the Riemann tensor continues to be constructed via

$$R^{\rm GW}_{\alpha\beta\gamma\delta}=\frac{1}{2}\frac{\partial^2 h^{\rm TT}_{\{\alpha\beta}}{\partial\tau_r^2}k_\gamma k_{\delta\}}=\frac{1}{2}\frac{\partial^2 h^{\rm TT}_{\{\alpha\beta}}{\partial\tau_r^2}\frac{\partial\tau_r}{\partial x^\gamma}\frac{\partial\tau_r}{\partial x^{\delta\}}}\simeq\frac{1}{2}h^{\rm TT}_{\{\alpha\beta|\gamma\delta\}} \tag{26.82}$$

[Eq. (26.72)].

We shall now sketch a proof that this geometric-optics Riemann tensor does, indeed, satisfy the gravitational wave equation. The foundation for the proof is the geometric-optics condition that h_+, $h_\times$, and thence $R^{\rm GW}_{\alpha\beta\gamma\delta}$ are rapidly varying functions of retarded time τ_r and slowly varying functions of (θ,ϕ,r). To take advantage of this, we shall use a prime to denote derivatives at fixed τ_r, so

$$R^{\rm GW}_{\alpha\beta\gamma\delta|\mu}=R^{\rm GW}_{\alpha\beta\gamma\delta,\tau_r}\frac{\partial\tau_r}{\partial x_\mu}+R^{\rm GW}_{\alpha\beta\gamma\delta|\mu'}=-R^{\rm GW}_{\alpha\beta\gamma\delta,\tau_r}k_\mu+R^{\rm GW}_{\alpha\beta\gamma\delta|\mu'}\ . \tag{26.83}$$

Taking the divergence of this on the μ index we obtain

$$R^{\rm GW}_{\alpha\beta\gamma\delta|\mu}{}^{\mu} = R^{\rm GW}_{\alpha\beta\gamma\delta,\tau_r\tau_r}k_\mu k^\mu - 2R^{\rm GW}_{\alpha\beta\gamma\delta,\tau_r|\mu'}k^\mu - R^{\rm GW}_{\alpha\beta\gamma\delta,\tau_r}k_\mu{}^{|\mu} + R^{\rm GW}_{\alpha\beta\gamma\delta|\mu'}{}^{\mu'} \ . \tag{26.84}$$

In the limit as the waves' wavelength goes to zero, the first term á priori scales as $1/\lambda\!\!\!^{-2}$, the second and third as $1/\lambda\!\!\!^{-}$, and the fourth as $1/\lambda\!\!\!^{-0} = 1$. In the spirit of geometric optics (Sec. 6.3), we neglect the tiny third term. The leading-order, first term vanishes because $\vec{k}$ is null, so Eq. (26.84) reduces to

$$R^{\rm GW}_{\alpha\beta\gamma\delta|\mu}{}^{\mu} = -2R^{\rm GW}_{\alpha\beta\gamma\delta,\tau_r|\mu'}k^\mu - R^{\rm GW}_{\alpha\beta\gamma\delta,\tau_r}k_\mu{}^{|\mu} \tag{26.85}$$

The second term is the directional derivative of $-2R^{\rm GW}_{\alpha\beta\gamma\delta,\tau_r}$ along $\vec{k}$, i.e. along a ray. Since each ray has constant (θ,ϕ,τ_e), and since the vectors $\vec{a}$, $\vec{b}$, and $\vec{k}$ that appear in Eqs. (26.80)–(26.82) for $R^{\rm GW}_{\alpha\beta\gamma\delta}$ all are parallel transported along $\vec{k}$, the only piece of $R^{\rm GW}_{\alpha\beta\gamma\delta}$ that can vary along $\vec{k}$ is the factor $1/r$. Correspondingly,

$$R^{\rm GW}_{\alpha\beta\gamma\delta,\tau_r|\mu'}k^\mu = R^{\rm GW}_{\alpha\beta\gamma\delta,\tau_r}r\nabla_{\vec{k}}\left(\frac{1}{r}\right) \ . \tag{26.86}$$

Inserting this into Eq. (26.85) and invoking the propagation law (26.77) for r, we obtain

$$R^{\rm GW}_{\alpha\beta\gamma\delta|\mu}{}^{\mu} = 0 \ . \tag{26.87}$$

Thus, our geometric-optics formulae for $R^{\rm GW}_{\alpha\beta\gamma\delta}$ do, indeed, produce a solution to the gravitational wave equation. Moreover, since, in the source's local asymptotic rest frame, this solution reduces to the one developed in Sec. 26.3.5, the formulae for $R^{\rm GW}_{\alpha\beta\gamma\delta}$ also satisfy the gravitational wave equation.

26.3.7 Metric perturbation; TT gauge

Although the properties of gravitational waves and their propagation are best described in terms of the waves' Riemann tensor $R^{\rm GW}_{\alpha\beta\gamma\delta}$, their generation is best described in terms of the waves' metric perturbation $h_{\mu\nu}$ [cf. the linearized-theory analysis in Sec. 24.9.2]. As in linearized theory, so also here, there is gauge freedom in the waves' metric perturbation, which results from introducing a tiny, rippled displacement $\vec{\xi}$ of the coordinate lines. In a local Lorentz frame of the smooth background, the gauge change has the linearized-theory form $\delta h_{\mu\nu} = -\xi_{\mu,\nu} - \xi_{\nu,\mu}$ [Eq. (24.104)], so in an arbitrary coordinate system of the background spacetime it must be

$$h^{\rm new}_{\mu\nu} = h^{\rm old}_{\mu\nu} - \xi_{\mu|\nu} - \xi_{\nu|\mu} \ . \tag{26.88}$$

By choosing the background coordinates to be local Lorentz and carefully adjusting the waves' gauge, we can ensure that the waves' metric perturbation is equal to the transverse-traceless gravitational-wave field (26.43), which we originally defined in terms of the Riemann tensor; i.e., we can ensure that

$$\begin{aligned} &h_{\alpha\beta} = h^{\rm TT}_{\alpha\beta} \ , \quad \text{or equivalently,} \\ &h_{xx} = -h_{yy} = h_+(t-z) \ , \quad h_{xy} = h_{yx} = h_\times(t-z) \ , \quad \text{all other } h_{\alpha\beta} \text{ vanish.} \end{aligned} \tag{26.89}$$

To see that this is possible, we need only verify that this metric perturbation produces the correct components of Riemann, Eq. (5.12a); indeed it does, as we can see by inserting Eqs. (26.89) into expression (26.26) for the Riemann tensor. For an alternative proof see Ex. 26.6. The gauge in which the waves' metric perturbation takes the simple TT form (26.89) is called *transverse-traceless gauge*, or TT gauge, and the coordinates in which the metric perturbation takes this form are called *TT coordinates*.

TT gauge is not the only one in which the waves' metric perturbation has the plane-wave form $h_{\alpha\beta} = h_{\alpha\beta}(t-z)$ There are many other such gauges; cf. Ex. 26.6. In any local Lorentz frame of the background spacetime and any gauge for which $h_{\alpha\beta} = h_{\alpha\beta}(t-z)$, the transverse components of the waves' Riemann curvature tensor take the form [derivable from Eq. (24.51) or (24.96)]

$$R^{\rm GW}_{j0k0} = -\frac{1}{2}\frac{\partial^2 h_{jk}}{\partial t^2} \text{ for } j = x\,, y \text{ and } k = x\,, y\ . \tag{26.90}$$

By comparing with Eq. (26.41) we see that in such a gauge, the transverse part of the waves' metric perturbation must be equal to the TT gravitational-wave field:

$$h^{\rm TT}_{jk} = (h_{jk})^{\rm T}\ . \tag{26.91}$$

Here the T on the right-hand side means "throw away all components except those which are spatial and are transverse to the waves' propagation direction". Since $h^{\rm TT}_{jk}$ is trace-free as well as transverse, we are guaranteed that the transverse part of the metric perturbation h_{jk} will be trace-free; i.e. $h_{xx} + h_{yy} = 1$. To emphasize this trace-free property it is conventional to write Eq. (26.91) in the form

$$h^{\rm TT}_{jk} = (h_{jk})^{\rm TT}\ , \tag{26.92}$$

where the second T on the right-hand side means "remove the trace, if the trace is not already zero". To repeat, *Eq. (26.92) is true in any gauge where the waves' contribution to the metric has the "speed-of-light-propagation" form* $h_{\alpha\beta} = h_{\alpha\beta}(t-z)$.

If we rotate the spatial axes so the waves propagate along the unit spatial vector $\mathbf{n}$ instead of along $\vec{e}_z$, then the "speed-of-light-propagation" form of the metric becomes

$$h_{\alpha\beta} = h_{\alpha\beta}(t - \mathbf{n}\cdot\mathbf{x})\ , \tag{26.93}$$

and the extraction of the spatial, transverse-traceless part of this metric perturbation can be achieved with the aid of the projection tensor

$$P^{jk} \equiv \delta^{jk} - n^j\, n^k\ . \tag{26.94}$$

Specifically,

$$h^{\rm TT}_{jk} = (h_{jk})^{\rm TT} = P_j{}^l P_k{}^m h_{lm} - \frac{1}{2} P_{jk} P^{lm} h_{lm}\ . \tag{26.95}$$

Here the notation is that of Cartesian coordinates with $P_j{}^k = P^{jk} = P_{jk}$.

When analyzing gravitational wave generation, the quantity most easily computed is often the trace-reversed metric perturbation, in a gauge with speed-of-light propagation, so $\bar{h}_{\alpha\beta} = \bar{h}_{\alpha\beta}(t - \mathbf{n}\cdot\mathbf{x})$. Because the projection process (26.95) removes the trace (i.e., the

result is insensitive to the trace), and $\bar{h}_{jk}$ and h_{jk} differ only in their trace, we can compute the gravitational-wave field by direct TT projection of $\bar{h}_{jk}$ without bothering to evaluate h_{jk} first:

$$h^{\rm TT}_{jk} = (\bar{h}_{jk})^{\rm TT} = P_j{}^l P_k{}^m \bar{h}_{lm} - \frac{1}{2} P_{jk} P^{lm} \bar{h}_{lm} \ . \tag{26.96}$$

****

EXERCISES

Exercise 26.4 *Derivation: Behavior of h_+ and $h_\times$ under rotations and boosts*

(a) Derive the behavior (26.51) of h_+ and $h_\times$ under rotations in the transverse plane. [Hint: show that $\mathbf{e}^+ + i\mathbf{e}^\times$ rotates through 2ψ, and then write $h^{\rm GW}_{\alpha\beta}$ [Eq. (26.43)] in terms of $h_+ + ih_\times$ and $\mathbf{e}^+ - i\mathbf{e}^\times$.]

(b) Show that, with the orientations of spatial basis vectors described after Eq. (26.51), h_+ and $h_\times$ are unchanged by boosts.

Exercise 26.5 *Problem: Energy-Momentum Conservation in Geometric Optics Limit*
Near the end of Sec. 26.3.6, we proved that our geometric-optics formulae for $R^{\rm GW}_{\alpha\beta\gamma\delta}$ satisfy the gravitational wave equation. Use these same techniques to show that the gravitational stress-energy tensor (26.58), with h_+ and $h_\times$ given by the geometric-optics formulae (26.80), has vanishing divergence, $\vec{\nabla} \cdot \mathbf{T}^{\rm GW} = 0$.

Exercise 26.6 *Example: Transformation to TT Gauge*
Consider a plane gravitational wave propagating in the z-direction through a local Lorentz frame of the smooth background spacetime. Such a wave can be described by Linearized Theory. In Sec. 24.9.2 and Ex. 24.13 we showed that, by a careful choice of the four gauge-generating functions $\xi^\alpha(\mathcal{P})$, one can bring the trace-reversed metric perturbation into Lorentz gauge, so it satisfies the gauge condition $\bar{h}_{\alpha\beta,}{}^\beta = 0$ and the wave equation $\bar{h}_{\alpha\beta,\mu}{}^\mu = 0$, and thence has the form $\bar{h}_{\alpha\beta} = h_{\alpha\beta}(t-z)$. In general there are 10 independent components of $\bar{h}_{\alpha\beta}$, since it is a symmetric second-rank tensor, but the 4 gauge conditions reduce this from 10 to 6. *Thus, in general, the Lorentz-gauge metric perturbation for a plane gravitational wave contains six independent functions of $t-z$.* Only two of these six can represent physical degrees of freedom of the wave; the other four must be pure-gauge functions and must be removable by a further specialization of the gauge. This exercise explores that further gauge freedom.

(a) Consider any trace-reversed metric perturbation that is in Lorentz gauge. Show that a further gauge change whose generators satisfy the wave equation $\xi_{\alpha,\mu}{}^\mu = 0$ leaves $\bar{h}_{\alpha\beta}$ still in Lorentz gauge. Show that such a gauge change, in general, involves four free functions of *three* of the spacetime coordinates, by contrast with general gauge transformations which entail four free functions of all *four* spacetime coordinates.

(b) Consider the plane gravitational wave described in the first paragraph of this problem. Exhibit gauge-change generators ξ_α that satisfy the wave equation and that remove four of the six independent functions from $\bar{h}_{\alpha\beta}$, bringing it into TT gauge, so the components of $h_{\alpha\beta}$ are given by Eqs. (26.89).

(c) Show by an explicit calculation that the gauge change of part (b) can be achieved by throwing away all pieces of $h_{\alpha\beta}$ except the transverse ones (those that lie in the x-y plane) and by then removing the trace — i.e. by the transverse-traceless projection of Eq. (26.92).

****

26.4 The Generation of Gravitational Waves

26.4.1 Multipole-moment expansion

The electromagnetic waves emitted by a dynamical charge distribution are usually expressed as a sum over the source's multipole moments. There are two families of moments: the electric moments (moments of the electric charge distribution) and the magnetic moments (moments of the electric current distribution).

Similarly, the gravitational waves emitted by a dynamical distribution of mass-energy and momentum can be expressed as a sum over multipole moments. Again there are two families of moments: the *mass moments* (moments of the mass-energy distribution) and the *current moments* (moments of the mass-current distribution, i.e. the momentum distribution). The multipolar expansion of gravitational waves is presented in great detail in Thorne (1980). In this section we shall sketch and explain its qualitative and order-of-magnitude features.

In the source's weak-gravity near zone (if it has one), the mass moments show up in the time-time part of the metric in a form familiar from Newtonian theory

$$g_{00} = -(1+2\Phi) = -1 \& \frac{\mathcal{I}_0}{r} \& \frac{\mathcal{I}_1}{r^2} \& \frac{\mathcal{I}_2}{r^3} \& \dots \ . \tag{26.97}$$

[cf. Eq. (24.95)]. Here r is radius, $\mathcal{I}_\ell$ is the moment of order ℓ, and "&" means "plus terms with the form". The mass monopole moment $\mathcal{I}_0$ is the source's mass, and the mass dipole moment $\mathcal{I}_1$ can be made to vanish by placing the origin of coordinates at the center of mass.

Similarly, in the source's weak-gravity near zone, its current moments $\mathcal{S}_\ell$ show up in the space-time part of the metric

$$g_{0j} = \frac{\mathcal{S}_1}{r^2} \& \frac{\mathcal{S}_2}{r^3} \& \dots \ . \tag{26.98}$$

Just as there is no magnetic monopole moment in classical electromagnetic theory, so there is no current monopole moment in general relativity. The current dipole moment $\mathcal{S}_1$ is the source's angular momentum, so the leading-order term in the expansion (26.98) has the form (24.112), which we have used to deduce the angular momenta of gravitating bodies.

If the source has mass M, size L and internal velocities $\sim v$, then the magnitudes of its moments are

$$\mathcal{I}_\ell \sim ML^\ell \ , \quad \mathcal{S}_\ell \sim MvL^\ell \tag{26.99}$$

These formulae guarantee that the near-zone fields g_{00} and g_{0j}, as given by Eqs. (26.97) and (26.98), are dimensionless.

As the source's moments oscillate dynamically, they produce gravitational waves. Mass-energy conservation [Eq. (24.114)] prevents the mass monopole moment $\mathcal{I}_0 = M$ from oscillating; angular-momentum conservation [Eq. (24.115)] prevents the current dipole moment $\mathcal{S}_1$ = (angular momentum) from oscillating; and because the time derivative of the mass dipole moment $\mathcal{I}_1$ is the source's linear momentum, momentum conservation [Eq. (24.118)] prevents the mass dipole moment from oscillating. Therefore, the lowest-order moments that can contribute to the waves are the quadrupolar ones. The wave fields h_+ and $h_\times$ in the source's local asymptotic rest frame must (i) be dimensionless, (ii) die out as $1/r$, and (iii) be expressed as a sum over derivatives of the multipole moments. These conditions guarantee that the waves will have the following form:

$$h_+ \sim h_\times \sim \frac{\partial^2 \mathcal{I}_2/\partial t^2}{r} \& \frac{\partial^3 \mathcal{I}_3/\partial t^3}{r} \& \ldots \& \frac{\partial^2 \mathcal{S}_2/\partial t^2}{r} \& \frac{\partial^3 \mathcal{S}_3/\partial t^3}{r} \& \ldots \ . \tag{26.100}$$

The timescale on which the moments oscillate is $T \sim L/v$, so each time derivative produces a factor v/L. Correspondingly, the ℓ-pole contributions to the waves have magnitudes

$$\frac{\partial^\ell \mathcal{I}_\ell/\partial t^\ell}{r} \sim \frac{M}{r} v^\ell \ , \quad \frac{\partial^\ell \mathcal{S}_\ell/\partial t^\ell}{r} \sim \frac{M}{r} v^{(\ell+1)} \ . \tag{26.101}$$

This means that, for a "slow-motion source" (one with internal velocities v small compared to light so the reduced wavelength $\lambda\!\!\!^{-} \sim L/v$ is large compared to the source size L), *the mass quadrupole moment $\mathcal{I}_2$ will produce the strongest waves.* The mass octupole waves and current quadrupole waves will be weaker by $\sim v \sim L/\lambda\!\!\!^{-}$; the mass 4-pole and current octupole waves will be weaker by $\sim v^2 \sim \lambda\!\!\!^{-2}/L^2$, etc. This is analogous to the electromagnetic case, where the electric dipole waves are the strongest, the electric quadrupole and magnetic dipole are smaller by $\sim \lambda\!\!\!^{-}/L$, etc.

In the next section we shall develop the theory of mass-quadrupole gravitational waves. For the corresponding theory of higher-order multipoles, see, e.g., Sec. VIII of Thorne (1980).

26.4.2 Quadrupole-moment formalism

Consider a weakly gravitating, nearly Newtonian system, e.g. a binary star system, and write its Newtonian potential in the usual way

$$\Phi(\mathbf{x}) = -\int \frac{\rho(\mathbf{x}')}{|\mathbf{x}-\mathbf{x}'|} dV_{x'} \ . \tag{26.102}$$

By using Cartesian coordinates, placing the origin of coordinates at the center of mass, and expanding

$$\frac{1}{|\mathbf{x}-\mathbf{x}'|} = \frac{1}{r} + \frac{x^j x^{j'}}{r^3} + \frac{x^j x^k (3x^{j'}x^{k'} - r'^2 \delta_{jk})}{2r^5} + \ldots \ , \tag{26.103}$$

we obtain the multipolar expansion of the Newtonian potential

$$\Phi(\mathbf{x}) = -\frac{M}{r} - \frac{3\mathcal{I}_{jk}x^j x^k}{2r^5} + \dots \ . \tag{26.104}$$

Here

$$M = \int \rho dV_x \ , \quad \mathcal{I}_{jk} = \int \rho \left(x^j x^k - \frac{1}{3} r^2 \delta_{jk} \right) dV_x \tag{26.105}$$

are the system's mass and mass quadrupole moment. Note that *the mass quadrupole moment is equal to the second moment of the mass distribution, with its trace removed.*

As we have discussed, dynamical oscillations of the quadrupole moment produce gravitational waves. Those waves must be describable by an outgoing-wave solution to the Lorentz-gauge, linearized Einstein equations

$$\bar{h}_{\mu\nu,}{}^{\nu} = 0 \ , \quad \bar{h}_{\mu\nu,\alpha}{}^{\alpha} = 0 \tag{26.106}$$

[Eqs. (24.105) and (24.106)] that has the near-zone Newtonian limit

$$\frac{1}{2}(\bar{h}_{00} + \bar{h}_{xx} + \bar{h}_{yy} + \bar{h}_{zz}) = h_{00} = \frac{3\mathcal{I}_{jk}x^j x^k}{r} \tag{26.107}$$

[cf. Eq. (24.101)].

The desired solution can be written in the form

$$\bar{h}_{00} = 2\left[\frac{\mathcal{I}_{jk}(t-r)}{r}\right]_{,jk} \ , \quad \bar{h}_{0j} = 2\left[\frac{\dot{\mathcal{I}}_{jk}(t-r)}{r}\right]_{,k} \ , \quad \bar{h}_{jk} = 2\frac{\ddot{\mathcal{I}}_{jk}(t-r)}{r} \ , \tag{26.108}$$

where the coordinates are Cartesian, $r \equiv \sqrt{\delta_{jk}x^j x^k}$, and the dots denote time derivatives. To verify that this is the desired solution: (i) Compute its divergence $\bar{h}_{\alpha\beta,}{}^{\beta}$ and obtain zero almost trivially. (ii) Notice that each Lorentz-frame component of $\bar{h}_{\alpha\beta}$ has the form $f(t-r)/r$ aside from some derivatives that commute with the wave operator, which implies that it satisfies the wave equation. (iii) Notice that in the near zone, the slow-motion assumption inherent in the Newtonian limit makes the time derivatives negligible, so $\bar{h}_{jk} \simeq 0$ and $\bar{h}_{00}$ is twice the right-hand side of Eq. (26.107), as desired.

Because the trace-reversed metric perturbation (26.108) in the wave zone has the speed-of-light-propagation form, aside from its very slow decay as $1/r$, we can compute the gravitational-wave field $h^{\rm TT}_{jk}$ from it by transverse-traceless projection, Eq. (26.96) with $\mathbf{n} = \mathbf{e}_r$:

$$h^{\rm TT}_{jk} = 2\left[\frac{\ddot{\mathcal{I}}_{jk}(t-r)}{r}\right]^{\rm TT} \ . \tag{26.109}$$

This is called *the quadrupole-moment formula for gravitational-wave generation.* Our derivation shows that it is valid for any nearly Newtonian source. Looking back more carefully at the derivation, one can see that, in fact, it relied only on the linearized Einstein equations and the Newtonian potential in the source's local asymptotic rest frame. Therefore, this quadrupole formula is also valid for slow-motion sources that have strong internal gravity

(e.g., slowly spinning neutron stars), so long as we read the quadrupole moment $\mathcal{I}_{jk}(t-r)$ off the source's near-zone Newtonian potential (26.104) and don't try to compute it via the Newtonian volume integral (26.105).

When the source is nearly Newtonian, so the volume integral (26.105) can be used to compute the quadrupole moment, the computation of the waves is simplified by computing instead the second moment of the mass distribution

$$I_{jk} = \int \rho x^j x^k dV_x \ , \tag{26.110}$$

which differs from the quadrupole moment solely in its trace. Then, because the TT projection is insensitive to the trace, the wave field (26.109) can be computed as

$$h^{\rm TT}_{jk} = 2\left[\frac{\ddot{I}_{jk}(t-r)}{r}\right]^{\rm TT} \ . \tag{26.111}$$

To get an order of magnitude feeling for the strength of the gravitational waves, notice that the second time derivative of the quadrupole moment, in order of magnitude, is the nonspherical part of the source's internal kinetic energy, $E^{\rm ns}_{\rm kin}$, so

$$h_+ \sim h_\times \sim \frac{E^{\rm ns}_{\rm kin}}{r} = G\frac{E^{\rm ns}_{\rm kin}}{c^4 r} \ , \tag{26.112}$$

where the second expression is written in conventional units. Although this estimate is based on the slow-motion assumption of source size small compared to reduced wavelength, $L \ll \lambda\!\!\!^{-}$, it remains valid in order of magnitude when extrapolated into the realm of the strongest of all realistic astrophysical sources, which have $L \sim \lambda\!\!\!^{-}$. For sources in the "high-frequency" band of ground-based detectors (as we shall see below), the largest value of $E^{\rm ns}_{\rm kin}$ that is likely to occur is roughly $E^{\rm ns}_{\rm kin} \sim M_\odot \sim 1$ km, where $M_\odot$ is the mass of the Sun The collision of two smallish black holes (masses of several solar masses) will have such an $E^{\rm ns}_{\rm kin}$. Such a source at the center of our galaxy would produce $h_+ \sim 10^{-17}$; at the center of the Virgo cluster of galaxies it would produce $h_+ \sim 10^{-20}$, and at the Hubble distance (edge of the observable universe) it would produce $h_+ \sim 10^{-23}$. This sets the sensitivity goals of ground-based detectors, Sec. 26.5.

Because the gravitational stress-energy tensor $T^{\rm GW}_{\mu\nu}$ produces background curvature via the Einstein equation $G^{\rm B}_{\mu\nu} = 8\pi T^{\rm GW}_{\mu\nu}$, just like nongravitational stress-energy tensors, it must contribute to the rate of change of the source's mass M, linear momentum P_j and angular momentum S_j [Eqs. (24.114)–(24.118)] just like other stress-energies. When one inserts the quadrupolar $T^{\rm B}_{\mu\nu}$ into Eqs. (24.114)–(24.118) and integrates over a sphere in the wave zone of the source's local asymptotic rest frame, one finds that

$$\frac{dM}{dt} = -\frac{1}{5}\left\langle \frac{\partial^3 \mathcal{I}_{jk}}{\partial t^3}\frac{\partial^3 \mathcal{I}_{jk}}{\partial t^3}\right\rangle \ , \tag{26.113}$$

$$\frac{dS_i}{dt} = -\frac{2}{5}\epsilon_{ijk}\left\langle \frac{\partial^2 \mathcal{I}_{jm}}{\partial t^2}\frac{\partial^3 \mathcal{I}_{km}}{\partial t^3}\right\rangle \ , \tag{26.114}$$

and $dP_j/dt = 0$. It turns out [cf. Sec. IV of Thorne (1980)] that the dominant linear-momentum change (i.e., the dominant radiation-reaction "kick") arises from a beating of the mass quadrupole moment against the mass octupole moment, and mass quadrupole against current quadrupole.

The back reaction of the emitted waves on their source shows up not only in changes of the source's mass, momentum, and angular momentum, but also in accompanying changes of the source's internal structure. These structure changes can be deduced fully, in many cases, from dM/dt, dS_j/dt and dP_j/dt. A nearly Newtonian binary system is an example (Sec. 26.4.3 below). However, in other cases (e.g., a compact body orbiting near the horizon of a black hole), the only way to compute the structure changes is via a *gravitational-radiation-reaction force* that acts back on the system.

The simplest example of such a force is one derived by William Burke (1971) for quadrupole waves emitted by a nearly Newtonian system. Burke's quadrupolar radiation-reaction force can be incorporated into Newtonian gravitation theory by simply augmenting the system's near-zone Newtonian potential by a radiation-reaction term, computed from the fifth time derivative of the system's quadrupole moment:

$$\Phi^{\rm react} = \frac{1}{5}\frac{\partial^5 \mathcal{I}_{jk}}{\partial t^5} x^j x^k \ . \tag{26.115}$$

This potential satisfies the vacuum Newtonian field equation $\nabla^2\Phi \equiv \delta_{jk}\Phi_{,jk} = 0$ because $\mathcal{I}_{jk}$ is trace free.

This augmentation onto the Newtonian potential arises as a result of general relativity's outgoing-wave condition. If one were to switch to an ingoing-wave condition, $\Phi^{\rm react}$ would change sign, and if the system's oscillating quadrupole moment were joined onto standing gravitational waves, $\Phi^{\rm react}$ would go away. In Ex. 26.9, it is shown that the radiation reaction force density $-\rho\boldsymbol{\nabla}\Phi^{\rm react}$ saps energy from the system at the same rate as the gravitational waves carry it away.

Burke's gravitational radiation-reaction potential $\Phi^{\rm react}$ and force density $-\rho\boldsymbol{\nabla}\Phi^{\rm react}$ are close analogs of the radiation reaction potential [last term in Eq. (15.92)] and acceleration [right side of Eq. (15.95)] that act on an oscillating ball which emits sound waves into a surrounding fluid. Moreover, Burke's derivation of his gravitational radiation-reaction potential is conceptually the same as the derivation, in Chap. 15, of the sound-wave reaction potential.

26.4.3 Gravitational waves from a binary star system

A very important application of the quadrupole formalism is to wave emission by a nearly Newtonian binary star system. Denote the stars by indices A and B and their masses by of the binary's two stars be M_A and M_B, so their total and reduced mass are (as usual)

$$M = M_A + M_B \ , \quad \mu = \frac{M_A M_B}{M} \ ; \tag{26.116}$$

and let the binary's orbit be circular, for simplicy, with separation a between the stars' centers of mass. Then Newtonian force balance dictates that the orbital angular velocity Ω

is given by Kepler's law,

$$\Omega = \sqrt{M/a^3}\ . \tag{26.117}$$

and the orbits of the two stars are

$$x_A = \frac{M_B}{M} a\cos\Omega t\ , \quad y_A = \frac{M_B}{M} a\sin\Omega t\ , \quad x_B = -\frac{M_A}{M} a\cos\Omega t\ , \quad y_B = -\frac{M_A}{M} a\sin\Omega t\ . \tag{26.118}$$

The second moment of the mass distribution, Eq. (26.110), is $I_{jk} = M_A x_A^j x_A^k + M_B x_B^j x_B^k$. Inserting the stars' time-dependent positions (26.118), we obtain as the only nonzero components

$$I_{xx} = \mu a^2 \cos^2\Omega t\ , \quad I_{yy} = \mu a^2 \sin^2\Omega t\ , \quad I_{xy} = I_{yx} = \mu a^2 \cos\Omega t \sin\Omega t\ . \tag{26.119}$$

Noting that $\cos^2\Omega t = \frac{1}{2}(1+\cos 2\Omega t)$, $\sin^2\Omega t = \frac{1}{2}(1-\cos 2\Omega t)$ and $\cos\Omega t\sin\Omega t = \frac{1}{2}\sin 2\Omega t$, and evaluating the double time derivative, we obtain

$$\begin{aligned} \ddot{I}_{xx} &= -2\mu(M\Omega)^{2/3}\cos 2\Omega t\,, \quad \ddot{I}_{yy} = 2\mu(M\Omega)^{2/3}\cos 2\Omega t\,, \\ \ddot{I}_{xy} &= \ddot{I}_{yx} = -2\mu(M\Omega)^{2/3}\sin 2\Omega t\,. \end{aligned} \tag{26.120}$$

We express this in terms of Ω rather than a because Ω is a direct gravitational-wave observable: the waves' angular frequency is 2Ω.

To compute the gravitational-wave field (26.109), we must project out the transverse part of this. The projection is best performed in an orthonormal spherical basis, since there the transverse part is just the projection into the plane spanned by $\vec{e}_{\hat\theta}$ and $\vec{e}_{\hat\phi}$, and the transverse-traceless part just has components

$$(\ddot{I}_{\hat\theta\hat\theta})^{\rm TT} = -(\ddot{I}_{\hat\phi\hat\phi})^{\rm TT} = \frac{1}{2}(\ddot{I}_{\hat\theta\hat\theta} - \ddot{I}_{\hat\phi\hat\phi})\ , \quad (\ddot{I}_{\hat\theta\hat\phi})^{\rm TT} = \ddot{I}_{\hat\theta\hat\phi}\ . \tag{26.121}$$

Now, a little thought will save us much work: We need only compute these quantities at $\phi = 0$ (i.e., in the x-z plane), since their circular motion guarantees that their dependence on t and ϕ must be solely through the quantity $\Omega t - \phi$. At $\phi = 0$, $\vec{e}_{\hat\theta} = \vec{e}_x\cos\theta - \vec{e}_z\sin\theta$ and $\vec{e}_{\hat\phi} = \vec{e}_y$, so the only nonzero components of the transformation matrices from the Cartesian basis to the transverse part of the spherical basis are $L^x{}_{\hat\theta} = \cos\theta$, $L^z{}_{\hat\theta} = -\sin\theta$, $L^y{}_{\hat\phi} = 1$. Using this transformation matrix, we obtain, at $\phi = 0$, $\ddot{I}_{\hat\theta\hat\theta} = \ddot{I}_{xx}\cos^2\theta$, $\ddot{I}_{\hat\phi\hat\phi} = \ddot{I}_{yy}$, $\ddot{I}_{\hat\theta\hat\phi} = \ddot{I}_{xy}\cos\theta$. Inserting these and expressions (26.120) into Eq. (26.124), and setting $\Omega t \to \Omega t - \phi$ to make the formulae valid away from $\phi = 0$, we obtain

$$\begin{aligned} (\ddot{I}_{\hat\theta\hat\theta})^{\rm TT} &= -(\ddot{I}_{\hat\phi})^{\rm TT} = -(1+\cos^2\theta)\ \mu(M\Omega)^{2/3}\cos[2(\Omega t-\phi)]\ . \\ (\ddot{I}_{\hat\theta\hat\phi})^{\rm TT} &= +(\ddot{I}_{\hat\phi\hat\theta})^{\rm TT} = -2\cos\theta\ \mu(M\Omega)^{2/3}\sin[2(\Omega t-\phi)]\ . \end{aligned} \tag{26.122}$$

The gravitational-wave field (26.109) is $2/r$ times this quantity evaluated at the retarded time $t - r$.

We shall make the conventional choice for the polarization tensors:

$$\mathbf{e}^+ = (\vec{e}_{\hat\theta}\otimes\vec{e}_{\hat\theta} - \vec{e}_{\hat\phi}\otimes\vec{e}_{\hat\phi})\ , \quad \mathbf{e}^\times = (\vec{e}_{\hat\theta}\otimes\vec{e}_{\hat\phi} + \vec{e}_{\hat\phi}\otimes\vec{e}_{\hat\theta})\ . \tag{26.123}$$

Then the two scalar gravitational-wave fields are

$$h_+ = h^{\rm TT}_{\hat\theta\hat\theta} = \frac{2}{r}[\ddot I_{\hat\theta\hat\theta}(t-r)]^{\rm TT} = -2(1+\cos^2\theta)\,\frac{\mu(M\Omega)^{2/3}}{r}\cos[2(\Omega t - \Omega r - \phi)]\ ,$$
$$h_\times = h^{\rm TT}_{\hat\theta\hat\phi} = \frac{2}{r}[\ddot I_{\hat\theta\hat\phi}(t-r)]^{\rm TT} = -4\cos\theta\,\frac{\mu(M\Omega)^{2/3}}{r}\sin[2(\Omega t - \Omega r - \phi)]\ . \qquad (26.124)$$

We have expressed the ampitudes of these waves in terms of the dimensionless quantity $(M\Omega)^{2/3} = M/a = v^2$, where v is the relative velocity of the two stars.

Notice that, as viewed from the polar axis $\theta = 0$, h_+ and $h_\times$ are identical except for a $\pi/2$ phase delay, which means that the net stretch-squeeze ellipse (the combination of those in Figs. 26.1 and 26.2) rotates with angular velocity Ω. This is the gravitational-wave variant of circular polarization and arises because the binary motion as viewed from the polar axis looks circular. By contrast, as viewed by an observer in the equatorial plane $\theta = \pi/2$, $h_\times$ vanishes, so the net stretch-sqeeze ellipse just oscillates along the + axes and the waves have linear polarization. This is natural, since the orbital motion as viewed by an equatorial observer is just a linear, horizontal, back-and-forth oscillation. Notice also that it the gravitational-wave frequency is twice the orbital frequency, i.e.

$$f = 2\frac{\Omega}{2\pi} = \frac{\Omega}{\pi}\ . \qquad (26.125)$$

To compute, via Eqs. (26.113) and (26.114), the rate at which energy and angular momentum are lost from the binary, we need to know the double and triple time derivatives of its quadrupole moment $\mathcal{I}_{jk}$. The double time derivative is just $\ddot I_{jk}$ with its trace removed, but Eq. (26.119) shows that $\ddot I_{jk}$ is already trace free so $\ddot{\mathcal{I}}_{jk} = \ddot I_{jk}$. Inserting Eq. (26.119) for this quantity into Eqs. (26.113) and (26.114) and performing the average over a gravitational-wave period, we find that

$$\frac{dM}{dt} = -\frac{32}{\pi}\frac{\mu^2}{M^2}(M\Omega)^{10/3}\ , \quad \frac{dS_z}{dt} = -\frac{1}{\Omega}\frac{dM}{dt}\ , \quad \frac{dS_x}{dt} = \frac{dS_y}{dt} = 0\ . \qquad (26.126)$$

This loss of energy and angular momentum causes the binary to spiral inward, decreasing the stars' separation a and increasing the orbital angular velocity Ω. By comparing Eqs. (26.126) with the standard equations for the binary's orbital energy and angular momentum, M − (sum of rest masses of stars) $= E = -\frac{1}{2}\mu M/a = -\frac{1}{2}\mu(M\Omega)^{2/3}$, and $S_z = \mu a^2\Omega = \mu(M\Omega)^{2/3}/\Omega$, we obtain an equation for $d\Omega/dt$ which we can integrate to give

$$\Omega = \pi f = \left(\frac{5}{256}\frac{1}{\mu M^{2/3}}\frac{1}{t_o - t}\right)^{3/8}\ . \qquad (26.127)$$

Here t_o (an integration constant) is the time remaining until the two stars merge, if the stars are thought of as point masses so their surfaces do not collide sooner. This equation can be inverted to read off the time until merger as a function of gravitational-wave frequency.

These results for a binary's waves and radiation-reaction-induced inspiral are of great importance for gravitational-wave detection; see, e.g., Cutler and Thorne (2002).

As the stars spiral inward, $(M\Omega)^{2/3} = M/a = v^2$ grows larger, h_+ and $h_\times$ grow larger, and relavistic corrections to our Newtonian, quadrupole analysis grow larger. Those relativistic

corrections (including current-quadrupole waves, mass-octupole waves, etc.) can be computed using a *post-Newtonian* expansion of the Einstein field equations, i.e. an expansion in $M/a \sim v^2$. The expected accuracies of the LIGO/VIRGO network require that, for neutron-star binaries, the expansion be carried to order v^6 beyond our Newtonian, quadrupole analysis!

At the end of the inspiral, the binary's stars (or black holes) come crashing together. To compute the waves from this final merger, with an accuracy comparable to the expected observations, it is necessary to solve the Einstein field equation on a computer. The techniques for this are called *numerical relativity*. Numerical relativity is currently in its infancy, but has great promise for producing new insights into general relativity.

****

EXERCISES

Exercise 26.7 *Example: Quadrupolar wave generation in linearized theory*
Derive the quadrupolar wave-generation formula (26.111) for a slow-motion, weak-gravity source in linearized theory, in Lorenz gauge, beginning with the retarded-integral formula

$$\bar{h}_{\mu\nu}(t,\mathbf{x}) = \int \frac{4T_{\mu\nu}(t-|\mathbf{x}-\mathbf{x}'|,\mathbf{x}'])}{|\mathbf{x}-\mathbf{x}'|} dV_{x'} \tag{26.128}$$

[Eq. (24.107)]. Your derivation might proceed as follows:

(a) Show that for a slow-motion source, the retarded integral gives for the $1/r \equiv 1/|\mathbf{x}|$ (radiative) part of $\bar{h}_{jk}$

$$\bar{h}_{jk}(t,\mathbf{x}) = \frac{4}{r}\int T_{jk}(t-r,\mathbf{x}')dV_{x'} \ . \tag{26.129}$$

(b) Show that in linearized theory in Lorenz gauge, the vacuum Einstein equations $-\bar{h}_{\mu\nu,\alpha}{}^{\alpha} = 16\pi T_{\mu\nu}$ [Eq. (24.106)] and the Lorenz gauge condition $\bar{h}_{\mu\nu,}{}^{\nu} = 0$ [Eq. (24.105)] together imply that the stress-energy tensor that generates the waves must have vanishing coordinate divergence, $T^{\mu\nu}{}_{,\nu} = 0$. This means that linearized theory is ignorant of the influence of self gravity on the gravitating $T^{\mu\nu}$!

(c) Show that this vanishing divergence implies $[T^{00}x^jx^k]_{,00} = [T^{lm}x^jx^k]_{,ml} - 2[T^{lj}x^k + T^{lk}x^j]_{,l} + 2T^{jk}$.

(d) By combining the results of (a) and (c), deduce that

$$\bar{h}_{jk}(t,\mathbf{x}) = \frac{2}{r}\frac{d^2I_{jk}(t-r)}{dt^2} \ , \tag{26.130}$$

where I_{jk} is the second moment of the source's (Newtonian) mass-energy distribution $T^{00} = \rho$ [Eq. (26.110)].

(e) Noticing that the trace-reversed metric perturbation (26.130) has the "speed-of-light-propagation" form, deduce that the gravitational-wave field $h^{\rm TT}_{jk}$ can be computed from (26.130) by a transverse-traceless projection, Eq. (26.96).

Comment: Part (b) shows that this linearized-theory analysis is incapable of deducing the gravitational waves emitted by a source whose dynanmics is controlled by its self gravity, e.g., a nearly Newtonian binary star system. By contrast, the derivation of the quadrupole formula given in Sec. 26.4.2 is valid for any slow-motion source, regardless of the strength and roles of its internal gravity; see the discussion following Eq. (26.109).

Exercise 26.8 *Problem: Energy carried by gravitational waves*
Compute the net rate at which the quadrupolar waves (26.109) carry energy away from their source, by carrying out the surface integral (24.114) with T^{0j} being Isaacson's gravitational-wave energy flux (26.58). Your answer should be Eq. (26.113). [Hint: perform the TT projection in Cartesian coordinates using the projection tensor (26.94), and make use of the following integrals over solid angle on the unit sphere

$$\frac{1}{4\pi}\int n_i d\Omega = 0\ , \quad \frac{1}{4\pi}\int n_i n_j d\Omega = \frac{1}{3}\delta_{ij}\ , \quad \frac{1}{4\pi}\int n_i n_j n_k d\Omega\ = 0;\ ,$$
$$\frac{1}{4\pi}\int n_i n_j n_k n_l = \frac{1}{15}(\delta_{ij}\delta_{kl}+\delta_{ik}\delta_{jl}+\delta_{il}\delta_{jk}). \tag{26.131}$$

These relations should be obvious by symmetry, aside from the numerical factors out in front. Those factors are most easily deduced by computing the z components, i.e., by setting $i=j=k=l=z$ and using $n_z=\cos\theta$.]

Exercise 26.9 *Problem: Energy removed by gravitational radiation reaction*
Burke's radiation-reaction potential (26.115) produces a force per unit volume $-\rho\boldsymbol{\nabla}\Phi^{\rm react}$ on its nearly Newtonian source. If we multiply this force per unit volume by the velocity $\mathbf{v}=d\mathbf{x}/dt$ of the source's material, we obtain thereby a rate of change of energy per unit volume. Correspondingly, the net rate of change of the system's mass-energy must be

$$\frac{dM}{dt} = -\int \rho\mathbf{v}\cdot\boldsymbol{\nabla}\Phi^{\rm react} dV_x\ . \tag{26.132}$$

Show that, when averaged over a few gravitational-wave periods, this formula agrees with the rate of change of mass (26.113) that we derived by integrating the outgoing waves' energy flux.

Exercise 26.10 *Problem: Propagation of waves through an expanding universe*
As we shall see in Chap. 27, the following line element is a possible model for the large-scale structure of our universe:

$$ds^2 = b^2[-d\eta^2 + d\chi^2 + \chi^2(d\theta^2+\sin^2\theta d\phi^2)]\ , \quad \text{where} \quad b=b_o\eta^2 \tag{26.133}$$

and b_o is a constant with dimensions of length. This is an expanding universe with flat spatial slices $\eta=$ constant. Notice that the proper time measured by observers at rest in the

spatial coordinate system is $t = b_o \int \eta^2 d\eta = (b_o/3)\eta^3$. A nearly Newtonian, circular binary is at rest at $\chi = 0$ in an epoch when $\eta \sim \eta_o$. The coordinates of the binary's local asymptotic rest frame are (t, r, θ, ϕ) where $r = a\chi$ and the coordinates cover only a tiny region of the universe, $\chi \lesssim \chi_o \ll \eta_o$. The gravitational waves in this local asymptotic rest frame are described by the Eqs. (26.123) and (26.124); see also Sec. 26.3.5. Use geometric optics (Sec. 26.3.6) to propagate these waves out through the expanding universe. In particular

(a) Show that the null rays are the curves of constant θ, ϕ, and $\eta - \chi$.

(b) Show that the orthonormal basis vectors $\vec{e}_{\hat{\theta}}$, $\vec{e}_{\hat{\phi}}$ associated with the $(\eta, \chi, \theta, \phi)$ coordinates are parallel transported along the rays. (This should be fairly obvious from symmetry.)

(c) Show that the wave fields have the form (26.124) with $t - r$ replaced by the retarded time $\tau_r = \frac{1}{3} b_o (\eta - \chi)^3$, and with $1/r$ being some function of χ and η (what is that function?).

Exercise 26.11 *Problem: Gravitational waves emitted by a linear oscillator*
Consider a mass m attach to a spring so it oscillates along the z axis of a Cartesian coordinate system, moving along the world line $z = a \cos \Omega t$, $y = z = 0$. Use the quadrupole moment formalism to compute the gravitational waves $h_+(t, r, \theta, \phi)$ and $h_\times(t, r, \theta, \phi)$ emitted by this oscillator, with the polarization tensors chosen as in Eqs. (26.123). Pattern your analysis after the computation of waves from a binary in Sec. 26.4.3 .

Exercise 26.12 *Problem: Gravitational waves from waving arms*
Wave your arms rapidly, and thereby try to generate gravitational waves.

(a) Compute in order of magnitude, using classical general relativity, the wavelength of the waves you generate and their dimensionless amplitude at a distance of one wavelength away from you.

(b) How many gravitons do you produce per second? Discuss the implications of your result.

****

26.5 The Detection of Gravitational Waves

Physicists and astronomers are searching for gravitational waves in four different frequency bands using four different techniques:

- In the extremely low frequency (ELF) band, $\sim 10^{-15}$ to $\sim 10^{-18}$ Hz, gravitational waves are sought via their imprint on the polarization of the cosmic microwave background (CMB) radiation. There is only one expected ELF source of gravitational waves, but it is a very interesting one: quantum fluctuations in the gravitational field (spacetime

curvature) that emerge from the big bang's quantum-gravity regime, the *Planck era*, and that are subsequently amplified to classical, detectable sizes by the universe's early inflationary expansion. We shall study this amplification and the resulting ELF gravitational waves in Chap. 27 and shall see these waves' great potential for probing the physics of inflation.

- In the very low frequency (VLF) band, $\sim 10^{-7}$ to $\sim 10^{-9}$ Hz, gravitational waves are sought via their influence on the propagation of radio waves emitted by pulsars (spinning neutron stars) and by the resulting fluctuations in the arrival times of the pulsars' radio-wave pulses at earth. The expected VLF sources are violent processes in the first fraction of a second of the universe's life (Chap. 27), and the orbital motion of extremely massive pairs of black holes in the distant universe.

- In the low frequency (LF) band, $\sim 10^{-4}$ to ~ 0.1 Hz, gravitational waves are currently sought via their influence on the radio signals by which NASA tracks interplanetary spacecraft. In ~ 2012 this technique will be supplanted by LISA, the Laser Interferometer Space Antenna—three "drag-free" spacecraft in a triangular configuration with 5 kilometer long arms, that track each other via laser beams. LISA is likely to see waves from massive black-hole binaries (hole masses $\sim 10^5$ to $10^7 M_\odot$) out to cosmologiocal distances; from small holes, neutron stars, and white dwarfs spiraling into massive black holes out to cosmological distances; from the orbital motion of white-dwarf binaries, neutron-star binaries, and stellar-mass black-hole binaries in our own galaxy; and possibly from violent processes in the very early universe.

- The high frequency (HF) band, ~ 10 to $\sim 10^3$ Hz, is where earth-based detectors operate: laser interferometer gravitational wave detectors such as LIGO, and resonant-mass detectors in which a gravitational wave alters the amplitude and phase of vibrations of a normal mode of a large, cylindrical bar. These detectors are likely to see waves from spinning, slightly deformed neutron stars in our own galaxy, and from a variety of sources in the distant universe: the final inspiral and collisions of binaries made from neutron stars and/or stellar-mass black holes (up to hundreds of solar masses); the tearing apart of a neutron star by the spacetime curvature of a companion black hole; supernovae and the triggers of gamma ray bursts; and possibly waves from violent processes in the very early universe.

For detailed discussions of these gravitational-wave sources in all four frequency bands, and of prospects for their detection, see e.g. Cutler and Thorne (2002) and references therein. It is likely that waves will be seen in all four bands within the next 20 years, and the first detection is likely to occur in the HF band using gravitational-wave interferometers such as LIGO.

We briefly discussed such interferometers in Sec. 8.5, focusing on optical interferometry issues. In this chapter we shall analyze the interaction of a gravitational wave with such an interferometer. That analysis will not only teach us much about gravitational waves, but will also illustrate some central issues in the physical interpretation of general relativity theory.

To get quickly to the essentials, we shall examine initially a rather idealized detector: A Michaelson interferometer (one without the input mirrors of Fig. 8.11) that floats freely in

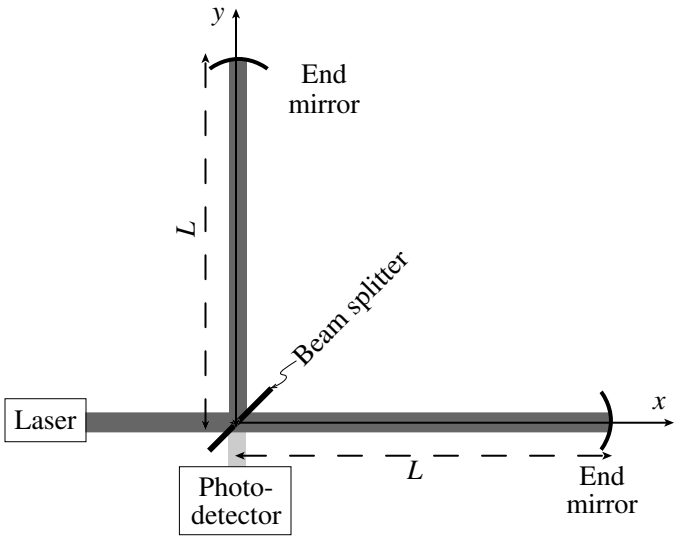

Fig. 26.3: An idealized gravitational-wave interferometer

space, so there is no need to hang its mirrors by wires; see Fig. 26.3. At the end of this chapter, we shall briefly discuss more realistic interferometers and their analysis.

We shall use linearized theory to analyze the interaction of our idealized interferometer with a gravitational wave. We shall perform our analysis twice, using two different coordinate systems (two different gauges). Our two analyses will predict the same results for the interferometer output, but they will appear to attribute those results to two different mechanisms.

In our first analysis (performed in TT gauge; Sec. 26.5.1) the interferometer's test masses will remain always at rest in our chosen coordinate system, and the gravitational waves $h_+(t-z)$ will interact with the interferometer's light. The imprint that $h_+(t-z)$ leaves on the light will cause a fluctuating light intensity $I_{\rm out}(t) \propto h_+(t)$ to emerge from the interferometer's output port and be measured by the photodiode.

In our second analysis (performed in the proper reference frame of the interferometer's beam splitter; Sec. 26.5.2) the gravitational waves will interact hardly at all with the light. Instead, they will push the end mirrors back and forth relative to the coordinate system, thereby lengthening one arm while shortening the other. These changing arm lengths will cause a changing interference of the light returning to the beam splitter from the two arms, and that changing interference will produce the fluctuating light intensity $I_{\rm out}(t) \propto h_+(t)$ measured by the photodiodes.

These differences of viewpoint are somewhat like the differences between the Heisenberg Picture and the Schroedinger Picture in quantum mechanics. The intuitive pictures associated with two viewpoints appear to be very different (Schroedinger's wave function vs. Heisenberg's matrices; gravitational waves interacting with light vs. gravitational waves pushing on mirrors). But whenever one computes the same physical observable from the two different viewpoints (probability for a quantum measurement outcome; light intensity measured by photodetector), the two viewpoints give the same answer.

26.5.1 Interferometer analyzed in TT gauge

For our first analysis, we place the interferometer at rest in the x-y plane of a TT coordinate system, with its arms along the x and y axes and its beam splitter at the origin as shown in Fig. 26.3. For simplicity, we assume that the gravitational wave propagates in the z direction and has + polarization, so the linearized spacetime metric has the TT-gauge form

$$ds^2 = -dt^2 + [1 + h_+(t-z)]dx^2 + [1 - h_+(t-z)]dy^2 + dz^2 \tag{26.134}$$

[Eq. (26.89)]. For ease of notation, we shall omit the subscript + from h_+ in the remainder of this section.

The beam splitter and end mirrors move freely and thus travel along geodesics of the metric (26.134). The splitter and mirrors are at rest in the TT coordinate system before the wave arrives, so initially the spatial components of their 4-velocities vanish, $u_j = 0$. Because the metric coefficients $g_{\alpha\beta}$ are all independent of x and y, the geodesic equation dictates that the components u_x and u_y are conserved and thus remain zero as the wave passes, which implies (since the metric is diagonal) $u^x = dx/d\tau = 0$ and $u^y = dy/d\tau = 0$. One can also show (see Ex. 26.13) that $u^z = dz/d\tau = 0$ throughout the wave's passage. Thus, in terms of motion relative to the TT coordinate system, the gravitational wave has no influence at all on the beam splitter and mirrors; they all remain at rest (constant x, y and z) as the waves pass.

(Despite this lack of motion, the proper distances between the mirrors and the beam splitter—the interferometer's physically measured arm lengths—do change. If the unchanging coordinate lengths of the two arms are $\Delta x = \ell_x$ and $\Delta y = \ell_y$, then the metric (26.134) says that the physically measured arm lengths are

$$L_x = \left[1 + \frac{1}{2}h(t)\right]\ell_x\ , \quad L_y = \left[1 - \frac{1}{2}h(t)\right]\ell_y\ . \tag{26.135}$$

When h is positive, the x arm is lengthened and the y arm is shortened; when negative, L_x is shortened and L_y is lengthened.)

Turn, next, to the propagation of light in the interferometer. We assume, for simplicity, that the light beams have large enough transverse sizes that we can idealize them, on their optic axes, as plane electromagnetic waves. (In reality, they will be Gaussian beams, of the sort studied in Sec. 7.5.5). The light's vector potential satisfies the curved-spacetime vacuum wave equation $A^{\alpha;\mu}{}_{\mu} = 0$ [Eq. (24.71) with vanishing Ricci tensor]. We write the vector potential in geometric optics (eikonal-approximation) form as

$$A^\alpha = \Re(\mathcal{A}^\alpha e^{i\phi})\ , \tag{26.136}$$

where $\mathcal{A}^\alpha$ is a slowly varying amplitude and ϕ is a rapidly varying phase; cf. Eq. (6.18). Because the wavefronts are (nearly) planar and the spacetime metric is nearly flat, the light's amplitude $\mathcal{A}^\mu$ will be very nearly constant as it propagates down the arms, and we can ignore its variations. Not so the phase. It oscillates at the laser frequency, $\omega_o \sim 3\times10^{14}$ Hz; i.e., $\phi^{\rm out}_{x\ {\rm arm}} \simeq \omega_o(x-t)$ for light propagating outward from the beam splitter along the x arm, and similarly for the returning light and the light in the y arm. The gravitational

wave imprints onto the phase tiny deviations from this $\omega_o(x-t)$; we must compute those imprints.

In the spirit of geometric optics, we introduce the light's spacetime wave vector

$$\vec{k} \equiv \vec{\nabla}\phi \ , \tag{26.137}$$

and we assume that $\vec{k}$ varies extremely slowly compared to the variations of ϕ. Then the wave equation $A^{\alpha;\mu}{}_{\mu} = 0$ reduces to the statement that the wave vector is null, $\vec{k}\cdot\vec{k} = \phi_{,\alpha}\phi_{,\beta}g^{\alpha\beta} = 0$. For light in the x arm the phase depends only on x and t; for that in the y arm it depends only on y and t. Combining this with the TT metric (26.134) and noting that the interferometer lies in the $z=0$ plane, we obtain

$$\begin{aligned} -\left(\frac{\partial\phi_{x\ \rm arm}}{\partial t}\right)^2 + [1-h(t)]\left(\frac{\partial\phi_{x\ \rm arm}}{\partial x}\right)^2 &= 0 \ , \\ -\left(\frac{\partial\phi_{y\ \rm arm}}{\partial t}\right)^2 + [1+h(t)]\left(\frac{\partial\phi_{y\ \rm arm}}{\partial y}\right)^2 &= 0 \ . \end{aligned} \tag{26.138}$$

We idealize the laser as perfectly monochromatic and we place it at rest in our TT coordinates, arbitrarily close to the beam splitter. Then the outgoing light frequency, as measured by the beam splitter, must be precisely ω_o and cannot vary with time. Since proper time, as measured by the beam splitter, is equal to coordinate time t [cf. the metric (26.134))], the frequency that the laser and beam splitter measure must be $\omega = -\partial\phi/\partial t = -k_t$. This dictates the following boundary conditions (initial conditions) on the phase of the light that travels outward from the beam splitter:

$$\frac{\partial\phi^{\rm out}_{x\ \rm arm}}{\partial t} = -\omega_o \text{ at } x=0 \ , \quad \frac{\partial\phi^{\rm out}_{y\ \rm arm}}{\partial t} = -\omega_o \text{ at } y=0 \ . \tag{26.139}$$

It is straightforward to verify that the solutions to Eq. (26.138) [and thence to the wave equation and thence to Maxwell's equation] that satisfy the boundary conditions (26.139) are

$$\begin{aligned} \phi^{\rm out}_{x\ \rm arm} &= -\omega_o\left[t - x + \frac{1}{2}H(t-x) - \frac{1}{2}H(t)\right] \ , \\ \phi^{\rm out}_{y\ \rm arm} &= -\omega_o\left[t - y - \frac{1}{2}H(t-y) + \frac{1}{2}H(t)\right] \ , \end{aligned} \tag{26.140}$$

where $H(t)$ is the first time integral of the gravitational waveform,

$$H(t) \equiv \int_0^t h(t')dt' \ ; \tag{26.141}$$

cf. Ex. 26.14.

The outgoing light reflects off the mirrors, which are at rest in the TT coordinates at locations $x=\ell_x$ and $y=\ell_y$. As measured by observers at rest in these coordinates, there

is no doppler shift of the light because the mirrors are not moving. Correspondingly, the phases of the reflected light, returning back along the two arms, have the following forms:

$$\begin{aligned}\phi^{\rm back}_{x\ {\rm arm}} &= -\omega_o\left[t+x-2\ell_x+\frac{1}{2}H(t+x-2\ell_x)-\frac{1}{2}H(t)\right]\ ,\\ \phi^{\rm back}_{y\ {\rm arm}} &= -\omega_o\left[t+y-2\ell_y-\frac{1}{2}H(t+y-2\ell_y)+\frac{1}{2}H(t)\right]\ .\end{aligned}\tag{26.142}$$

The difference of the phases of the returning light, at the beam splitter ($x=y=0$), is

$$\begin{aligned}\Delta\phi &\equiv \phi^{\rm back}_{x\ {\rm arm}}-\phi^{\rm back}_{y\ {\rm arm}}=-\omega_o[-2(\ell_x-\ell_y)+\frac{1}{2}H(t-2\ell_x)+\frac{1}{2}H(t-2\ell_y)-H(t)]\\ &\simeq +2\omega_o[\ell_x-\ell_y+\ell h(t)]\quad\text{for earth-based interferometers.}\end{aligned}\tag{26.143}$$

In the second line we have used the fact that for earth-based interferometers operating in the high-frequency band, the gravitational wavelength $\lambda_{\rm GW}\sim c/(100{\rm Hz})\sim 3000$ km is long compared to the interferometers' ~ 4 km arms, and the arms have nearly the same length, $\ell_y\simeq\ell_x\equiv\ell$.

The beam splitter sends a light field $\propto e^{i\phi^{\rm back}_{x\ {\rm arm}}}+e^{i\phi^{\rm back}_{y\ {\rm arm}}}$ back toward the laser, and a field $\propto e^{i\phi^{\rm back}_{x\ {\rm arm}}}-e^{i\phi^{\rm back}_{y\ {\rm arm}}}=e^{i\phi^{\rm back}_{y\ {\rm arm}}}(e^{i\Delta\phi}-1)$ toward the photodetector. The intensity of the light entering the photodetector is proportional to the squared amplitude of the field, $I_{\rm PD}\propto|e^{i\Delta\phi}-1|^2$. We adjust the interferometer's arm lengths so their difference $\ell_x-\ell_y$ is small compared to the light's reduced wavelength $1/\omega_o=c/\omega_o$ but large compared to $|\ell h(t)|$. Correspondingly, $|\Delta\phi|\ll 1$, so only a tiny fraction of the light goes toward the photodetector (it is the interferometer's "dark port"), and that dark-port light intensity is

$$I_{\rm PD}\propto|e^{i\Delta\phi}-1|^2\simeq|\Delta\phi|^2\simeq 4\omega_o^2(\ell_x-\ell_y)^2+8\omega_o^2(\ell_x-\ell_y)\ell h(t)\ .\tag{26.144}$$

The time varying part of this intensity is proportional to the gravitational waveform $h(t)$, and it is this time varying part that the photodetector reports as the interferometer output.

26.5.2 Interferometer analyzed in proper reference frame of beam splitter

We shall now reanalyze our idealized interferometer in the proper reference frame of its beam splitter, denoting that frame's coordinates by $\hat{x}^\alpha$. Because the beam splitter is freely falling (moving along a geodesic through the gravitational-wave spacetime), its proper reference frame is locally Lorentz ("LL"), and its metric coefficients have the form $g_{\hat\alpha\hat\beta}=\eta_{\alpha\beta}+{\rm O}(\delta_{jk}\hat{x}^j\hat{x}^k/\mathcal{R}^2)$ [Eq. (24.15)]. Here $\mathcal{R}$ is the radius of curvature of spacetime, and $1/\mathcal{R}^2$ is of order the components of the Riemann tensor, which have magnitude $\ddot{h}(\hat{t}-\hat{z})$ [Eq. (26.41) with t and z equal to $\hat{t}$ and $\hat{z}$ aside from fractional corrections of order h]. Thus,

$$g_{\hat\alpha\hat\beta}=\eta_{\alpha\beta}+{\rm O}[\ddot{h}(\hat{t}-\hat{z})\delta_{jk}\hat{x}^j\hat{x}^k]\ .\tag{26.145}$$

The following coordinate transformation takes us from the TT coordinates x^α used in the previous section to the beam splitter's LL coordinates:

$$x = \left[1 - \frac{1}{2}h(\hat{t}-\hat{z})\right]\hat{x}\ , \qquad y = \left[1 + \frac{1}{2}h(\hat{t}-\hat{z})\right]\hat{y}\ ,$$
$$t = \hat{t} - \frac{1}{4}\dot{h}(\hat{t}-\hat{z})(\hat{x}^2-\hat{y}^2)\ , \qquad z = \hat{z} + \frac{1}{4}\dot{h}(\hat{t}-\hat{z})(\hat{x}^2-\hat{y}^2)\ . \tag{26.146}$$

It is straightforward to insert this coordinate transformation into the TT-gauge metric (26.134) and thereby obtain, to linear order in h,

$$ds^2 = -d\hat{t}^2 + d\hat{x}^2 + d\hat{y}^2 + d\hat{z}^2 + \frac{1}{2}(\hat{x}^2-\hat{y}^2)\ddot{h}(t-z)(d\hat{t}-d\hat{z})^2\ . \tag{26.147}$$

This has the expected LL form (26.145) and, remarkably, it turns out not only to be a solution of the vacuum Einstein equations in linearized theory but also an exact solution to the full vacuum Einstein equations [cf. Ex. 35.8 of MTW].

Throughout our idealized interferometer, the magnitude of the metric perturbation in these LL coordinates is $|h_{\hat{\alpha}\hat{\beta}}| \lesssim (\ell/\lambda\!\!\!^{-}_{\rm GW})^2 h$, where $\lambda\!\!\!^{-}_{\rm GW} = \lambda_{\rm GW}/2\pi$ is the waves' reduced wavelength and h is the magnitude of $h(\hat{t}-\hat{z})$. For earth-based interferometers operating in the HF band (~ 10 to ~ 1000 Hz), $\lambda\!\!\!^{-}_{\rm GW}$ is of order 50 to 5000 km, and the arm lengths are $\ell \leq 4$ km, so $(L/\lambda\!\!\!^{-})^2 \lesssim 10^{-2}$ to 10^{-6}. Thus, the metric coefficients $h_{\hat{\alpha}\hat{\beta}}$ are no larger than $h/100$. This has a valuable consequence for the analysis of the interferometer: Up to fractional accuracy $\sim (\ell/\lambda\!\!\!^{-}_{\rm GW})^2 h \lesssim h/100$, the LL coordinates are globally Lorentz throughout the interferometer; i.e., $\hat{t}$ measures proper time, and $\hat{x}^j$ are Cartesian and measure proper distance. In the rest of this section, we shall restrict attention to such earth-based interfrometers, but shall continue to idealize them as freely falling.

The beam splitter, being initially at rest at the origin of these LL coordinates, remains always at rest, but the mirrors move. Not surprisingly, the geodesic equation for the mirrors in the metric (26.147) dictates that their coordinate positions are, up to fractional errors of order $(\ell/\lambda\!\!\!^{-}_{\rm GW})^2 h$,

$$\hat{x} = L_x = \left[1 + \frac{1}{2}h(\hat{t})\right]\ell_x\ , \quad \hat{y} = \hat{z} = 0 \quad \text{for mirror in } x \text{ arm},$$
$$\hat{y} = L_y = \left[[1 - \frac{1}{2}h(\hat{t})\right]\ell_y\ , \quad \hat{x} = \hat{z} = 0 \quad \text{for mirror in } y \text{ arm}. \tag{26.148}$$

(This can also be deduced from the gravitational-wave tidal acceleration $-R^{\rm GW}_{\hat{t}\hat{0}\hat{k}\hat{0}}\hat{x}^k$, as in Eq. (26.45), and from the fact that to good accuracy $\hat{x}$ and $\hat{y}$ measure proper distance from the beam splitter.) Thus, although the mirrors do not move in TT coordinates, they do move in LL coordinates. The two coordinate systems predict the same time-varying physical arm lengths (the same proper distances from beam splitter to mirrors), L_x and L_y [Eqs. (26.135) and (26.148)].

As in TT coordinates, so also in LL coordinates, we can analyze the light propagation in the geometric optics approximation, with $A^{\hat{\alpha}} = \Re(\mathcal{A}^{\hat{\alpha}} e^{i\phi})$. Just as the wave equation for the vector potential dictates, in TT coordinates, that the rapidly varying phase of the

outward light in the x arm has the form $\phi^{\rm out}_{x\ {\rm arm}} = -\omega_o(t-x) + {\rm O}(\omega_o \ell h_{\mu\nu})$ [Eq. (26.140) with $x \sim \ell \ll \lambda\!\!\!^{-}_{\rm GW}$ so $H(t-x) - H(t) \simeq \dot{H}(t)x = h(t)x \sim hL \sim h_{\mu\nu}L$], so similarly the wave equation in LL coordinates turns out to dictate that

$$\phi^{\rm out}_{x\ {\rm arm}} = -\omega_o(\hat{t}-\hat{x}) + {\rm O}(\omega_o \ell h_{\hat{\mu}\hat{\nu}}) = -\omega_o(\hat{t}-\hat{x}) + {\rm O}\left(\omega_o \ell h \frac{\ell^2}{\lambda\!\!\!^{-2}_{\rm GW}}\right) , \tag{26.149}$$

and similarly for the returning light and the light in the y arm. The term ${\rm O}(\omega_o \ell h\ \ell^2/\lambda\!\!\!^{-2}_{\rm GW})$ is the influence of the direct interaction between the gravitational wave and the light. Aside from this term, the analysis of the interferometer proceeds in exactly the same way as in flat space (because $\hat{t}$ measures proper time and $\hat{x}$ and $\hat{y}$ proper distance): The light travels a round trip distance L_x in one arm and L_y in the other, and therefore acquires a phase difference, upon arriving back at the beam splitter, given by

$$\begin{aligned} \Delta\phi &= -\omega_o[-2(L_x - L_y)] + {\rm O}\left(\omega_o \ell h \frac{\ell^2}{\lambda\!\!\!^{-2}_{\rm GW}}\right) \\ &\simeq +2\omega_o[\ell_x - \ell_y + \ell h(\hat{t})] + {\rm O}\left(\omega_o \ell h \frac{\ell^2}{\lambda\!\!\!^{-2}_{\rm GW}}\right) . \end{aligned} \tag{26.150}$$

This net phase difference for the light returning from the two arms is the same as we deduced in TT coordinates [Eq. (26.143)], up to the negligible correction ${\rm O}(\omega_o \ell h\ \ell^2/\lambda\!\!\!^{-2}_{\rm GW})$, and therefore the time-varying intensity of the light into the photodiode will be the same [Eq. (26.144)].

In our TT analysis the phase shift $2\omega_o \ell h(t)$ arose from the interaction of the light with the gravitational waves. In the LL analysis, it is due to the displacements of the mirrors in the LL coordinates (i.e., the displacements as measured in terms of proper distance), which cause the light to travel different distances in the two arms. The direct LL interaction of the waves with the light produces only the tiny correction ${\rm O}(\omega_o \ell h\ \ell^2/\lambda\!\!\!^{-2}_{\rm GW})$ to the phase shift.

It should be evident that the LL description is much closer to elementary physics than the TT description. This is always the case, when one's apparatus is sufficiently small that one can regard $\hat{t}$ as measuring proper time and $\hat{x}^j$ as Cartesian coordinates that measure proper distance throughout the apparatus. But for a large apparatus (e.g. LISA, with its arm lengths $\ell \gtrsim \lambda\!\!\!^{-}_{\rm GW}$) the LL analysis becomes quite complicated, as one must pay close attention to the ${\rm O}(\omega_o \ell h\ \ell^2/\lambda\!\!\!^{-2}_{\rm GW})$ corrections. In such a case, the TT analysis is much simpler.

26.5.3 Realistic Interferometers

For realistic, earth-based interferometers, one must take account of the acceleration of gravity. Experimenters do this by hanging their beam splitters and test masses on wires or fibers. The simplest way to analyze such an interferometer is in the proper reference frame of the beam splitter, where the metric must now include the influence of the acceleration of gravity by adding a term $-2g_e\hat{z}$ to the metric coefficient $h_{\hat{0}\hat{0}}$ [cf. Eq. (23.86)]. The resulting analysis, like that in the LL frame of our freely falling interferometer, will be identical to what one would do in flat spacetime, so long as one takes account of the motion of the test masses as dictated by the gravitational-wave tidal acceleration $-R_{\hat{i}\hat{0}\hat{j}\hat{0}}\hat{x}^j$, and so long as one is willing to ignore the tiny effects of ${\rm O}(\omega_o \ell h\ \ell^2/\lambda\!\!\!^{-2}_{\rm GW})$.

To make the realistic interferometer achieve high sensitivity, the experimenters introduce a lot of clever complications, such as the input mirrors of Fig. 8.11 which turn the arms into Fabry-Perot cavities. All these complications can be analyzed, in the beam splitter's proper reference frame, using standard flat-spacetime techniques, so long as one makes sure to take account of the end-mirror motion as dictated by the gravitational-wave tidal acceleeration. The direct coupling of the light to the gravitational waves can be neglected, as in our idealized interferometer.

****

EXERCISES

Exercise 26.13 *Derivation and Practice: Geodesic motion in TT coordinates*
Consider a particle that is at rest in the TT coordinate system of the gravitational-wave metric (26.134) before the gravitational wave arrives. In the text it is shown that the particle's 4-velocity has $u^x = u^y = 0$ as the wave passes. Show that $u^z = 0$ and $u^t = 1$ as the wave passes, so the components of the particle's 4-velocity are unaffected by the passing gravitational wave.

Exercise 26.14 *Example: Light in an interferometric gravitational wave detector in TT gauge*
Consider the light propagating outward from the beam splitter, along the x arm of an interferometric gravitational wave detector, as analyzed in TT gauge, so (suppressing the subscript "x arm" and superscript "out") the electromagnetic vector potential is $A^\alpha = \Re(\mathcal{A}^\alpha e^{i\phi(x,t)}$ with $\mathcal{A}^\alpha$ constant and with $\phi = -\omega_o \left[t - x + \frac{1}{2}H(t-x) - \frac{1}{2}H(t)\right]$ [Eqs. (26.140) and (26.141).

(a) Show that this ϕ satisfies the nullness equation (26.138), as claimed in the text — which implies that $A^\alpha = \Re(\mathcal{A}^\alpha e^{i\phi(x,t)})$ satisfies Maxwell's equations in the geometric optics limit.

(b) Show that this ϕ satisfies the initial condition (26.139), as claimed in the text.

(c) Show, by an argument analogous to Eq. (26.76), that $\nabla_{\vec{k}}\vec{k} = 0$. Thus, the wave vector must be the tangent vector to geometric optics rays that are null geodesics in the gravitational-wave metric. Photons travel along these null geodesics and have 4-momenta $\vec{p} = \hbar\vec{k}$.

(d) Because the gravitational-wave metric (26.134) is independent of x, the p_x component of a photon's 4-momentum must be conserved along its geodesic world line. Compute $p_x = k_x = -\partial\phi/\partial x$, thereby verify this conservation law.

(e) Explain why the photon's frequency, as measured by observers at rest in our TT coordinate system, is $\omega = -k_t = -\partial\phi/\partial t$. Explain why the rate of change of this frequency, as computed moving with the photon, is $d\omega/dt \simeq (\partial/\partial t + \partial/\partial x)\omega$, and show that $d\omega/dt \simeq -\frac{1}{2}\omega_o dh/dt$.

****

Bibliography

Bertotti, B., Iess, L. and Tortora, T., *Nature* **425**, 374 (2003).

Burke, William L., 1971. "Gravitational radiation damping of slowly moving systems calculated using matched asymptotic expansions," *Journal of Mathematical Physics*, **12**, 402–418.

Cutler, Curt and Thorne, Kip S., 2002. "An overview of gravitational wave sources," in Proceedings of the GR16 Conference on General Relativity and Gravitation, ed. N. Bishop and S. D. Maharaj (World Scientific, 2002), 72–111; also available at http://xxx.lanl.gov/abs/gr-qc/0204090

Einstein, Albert, 1916. "Die Grundlage der allgemeinen Relativitätstheorie," *Annalen der Physik*, **49**, 769–822. English translation in Einstein *et al*. (1923).

Einstein, Albert, 1918. "Über Gravitationwellen," *Sitzungsberichte der Königlish Preussischen Akademie der Wissenschaften*, **1918 volume**, 154–167.

Fierz, M. and Pauli, Wolfgang, 1939. "On relativistic wave equations for particles of arbitary spin in an electromagnetic field," *Proceedings of the Royal Society A*, **173**, 211–232.

Isaacson, R. A. 1968. *Physical Review* **166**, 1272.

MTW: Misner, Charles W., Thorne, Kip S. and Wheeler, John A., 1973. *Gravitation*, W. H. Freeman & Co., San Francisco.

Thorne, Kip S., 1980. *Review of Modern Physics*, **52**, 299.

Weissberg, J.M. and Taylor, J.H. in *Proceedings of the Aspen Conference on Binary Radio Pulsars*, eds. F.A. Rasio and I.H. Stairs (Astronomical Society of the Pacific Conference Series, in press); http://xxx.lanl.gov/abs/gr-qc/0407149 .

Will, Clifford M., 1993. *Theory and Experiment in Gravitational Physics*, Revised Edition, Cambridge University press, Cambridge, UK.

Will, Clifford M., 2001. "The Confrontation between General Relativity and Experiment," *Living Reviews in Relativity* **4**. [Online article]: cited on 18 May 2005, http://www.livingreviews.org/Irr-2001-4 .

Will, Clifford M., 2005. "Was Einstein Right? Testing Relativity at the Centenary," in *100 Years of Relativity: Spacetime Structure — Einstein and Beyond*, ed. A. Ashtekar, World Scientific, Singapore, in press. http://xxx.lanl.gov/abs/gr-qc/0504086

Contents

[3]MTW, Sec. 18.2 and Chap. 35, 36, 37; Thorne (1983, 1987).